Can Dynamic TDD Enabled Half-Duplex Cell-Free Massive MIMO Outperform Full-Duplex Cellular Massive MIMO?

Anubhab Chowdhury, Ribhu Chopra, and Chandra R. Murthy

***Abstract*—We consider a dynamic time division duplex (DTDD) enabled cell-free massive multiple-input multiple-output (CF-mMIMO) system, where each half-duplex (HD) access point (AP) is scheduled to operate in the uplink (UL) or downlink (DL) mode based on the data demands of the user equipments (UEs), with the goal of maximizing the sum UL-DL spectral efficiency (SE). We develop a new, low complexity, greedy algorithm for the combinatorial AP scheduling problem, with an optimality guarantee theoretically established via showing that a lower bound of the sum UL-DL SE is sub-modular. We also consider pilot sequence reuse among the UEs to limit the channel estimation overhead. In CF systems, all the APs estimate the channel from every UE, making pilot allocation problem different from the cellular case. We develop a novel algorithm that iteratively minimizes the maximum pilot contamination across the UEs. We compare the performance of our solutions, both theoretically and via simulations, against a full duplex (FD) multi-cell mMIMO system. Our results show that, due to the joint processing of the signals at the central processing unit, CF-mMIMO with dynamic HD AP-scheduling significantly outperforms cellular FD-mMIMO in terms of the sum SE and 90% likely SE. Thus, DTDD enabled HD CF-mMIMO is a promising alternative to cellular FD-mMIMO, without the cost of hardware for self-interference suppression.**

***Index Terms*—Cell-free massive MIMO, dynamic TDD, sub-modular optimization, pilot contamination.**

I. Introduction

In a cell free massive multiple-input multiple-output (CF-mMIMO) system, multiple access-points (APs) coherently and simultaneously serve a number of user equipments (UEs) distributed over a large geographical area [1]–[4]. Recently, CF-mMIMO has emerged as a promising candidate technology for the physical layer of next generation wireless communication systems [5]. It has been shown that under appropriate conditions [4], CF-mMIMO inherits many of the advantages offered by cellular massive MIMO such as channel hardening and favorable propagation. However, in their current form, CF-mMIMO systems are designed to work in the time division duplexed (TDD) mode, hence serving either only uplink (UL) or only downlink (DL) traffic at any given point in time. While enabling full duplex (FD) capabilities at the APs can simultaneously cater to the UL and DL data demands, the performance of such systems is limited by the residual self-interference (SI) power at each AP [6].

Anubhab Chowdhury and Chandra R. Murthy are with the Department of ECE, Indian Institute of Science, Bengaluru 560012, India. (e-mails:{anubhabc, cmurthy}@iisc.ac.in.)

Ribhu Chopra is with the Department of EEE, Indian Institute of Technology Guwahati, Assam 781039, India (e-mail: ribhufec@iitg.ac.in.)

This work was financially supported by research grants from the Prime Minister's Research Fellowship and the Young Faculty Research Fellowship awarded by the Govt. of India.

A. Motivation

In the context of cellular mMIMO, dynamic TDD (DTDD) has recently been explored to cater to heterogeneous UL-DL data demands from the UEs. This technique entails adaptive and independent splitting of the transmission frame into UL and DL slots by the different base stations (BSs) according to the UL-DL traffic demands from the UEs in each cell [7]. While this improves the overall spectral and time resource utilization across cells, it does not fully cater to heterogeneous data demands within the cells. That is, a UE with UL data demand will still have to wait for a slot where its serving BS is operating in the UL mode in order to complete its transmission, and similarly for a UE with DL data demand. On the other hand, in a CF-mMIMO system, since the UEs are not associated with a particular AP, if the APs can dynamically select the slots where they operate in UL and DL modes, any UE with a specific data demand can find some nearby APs operating in the corresponding mode in the same slot. Further, the joint processing of the signals at the CPU can mitigate the cross-link interferences (CLIs) that arise in a CF DTDD system. Due to this, a CF-mMIMO system with DTDD can potentially match or even exceed the performance of an FD-capable cellular system, while using half-duplex (HD) hardware at the APs. Therefore, the use of DTDD in conjunction with CF-mMIMO is the focus of this work.

B. Related Work

DTDD is a well accepted technique; it has been included in cellular communication standards such as 3GPP LTE Release 12 [8] and 5G NR [9], [10] to accommodate heterogeneous traffic loads. Traffic-dependent UL-DL slot adaptation schemes have been shown to reduce the overall system latency [11] and improve the spectral efficiency (SE) [12], [13] compared to TDD-based conventional cellular and CF mMIMO systems. However, the performance of DTDD is limited by two types of CLIs, namely, the interference from the DL BSs to the UL BSs and the interference from the UL UEs to the DL UEs. The CLI can be mitigated via intra cell-cooperation, power control and beamforming design, UE scheduling, etc. An excellent survey on the methods for CLI mitigation in cellular mMIMO can be found in [14].

On the other hand, FD technology can also serve UL and DL UEs simultaneously and has the potential to double the system capacity. Note that, in a cellular FD mMIMO system, similar CLIs exist as in DTDD based systems. However, in addition, each BS suffers from its own residual SI. In fact, the transmit RF-chain noise, oscillator phase noise, and related device imperfections get amplified while propagating through the SI channel and limit the FD system performance [6]. Also, the benefits of an FD cellular system considerably degrades under asymmetric traffic load [15]. In contrast, DTDD obviates the need for expensive and potentially power-hungry hardware as well as digital signal processing costs associated with SI mitigation. Numerical experiments have shown that the throughput of the cellular FD-system degrades relative to cellular DTDD as the UL-DL traffic asymmetry increases [16].

The current deployments of cellular DTDD require inter-cell cooperation, i.e., the neighboring cells need to exchange information (such as the estimated channel statistics or the per cell traffic load) for optimal UL-DL slot scheduling or interference mitigation. Although such techniques are attractive in theory, the sub-problems of BS/UE scheduling, power control, cell clustering [17], and joint beamformer design [18] are prohibitively complex for practical implementation. Moreover, the performance loss of the cell-edge UEs due to out-of-cell interference and CLI is a serious issue in cellular systems.

In contrast to cellular mMIMO, in a CF system, all the UEs in a given geographical area are served by all the available APs by jointly processing the signals to/from the UEs at a central processing unit (CPU). At the cost of a larger front-haul bandwidth, the CPU can utilize the knowledge of locally estimated channels from each AP to suppress the CLIs without inter-AP cooperation or extra signaling overhead [19]. Due to this, the quality of service (QoS) delivered is nearly uniform across all the UEs [3]. The advantages offered by DTDD along with the inherent benefits of the CF-architecture can be exploited to further enhance the system throughput under asymmetric traffic load. We not only dispense with the SI cancellation hardware at each AP; the computational burden and signaling overhead involved in CLI mitigation of a cellular mMIMO system is also considerably reduced at the CPU.

In the context of DTDD enabled CF-mMIMO systems, the authors in [19] presented a UE scheduling algorithm to alleviate the CLI from UL UEs to DL UEs. Recently, in [20], the authors proposed a so-called beamforming training based scheme, where the estimates of the effective DL channels are exploited to reduce inter-AP CLI. All the previous works assume a fixed UL and DL configuration across the APs, and focus primarily on CLI mitigation methods. However, unless the transmission and reception mode of each AP is dynamically adapted based on the traffic demands of the UEs, the benefits of DTDD cannot be fully exploited. Therefore, to enable DTDD, we need to split the time resources optimally at each of the APs. However, scheduling the APs via exhaustive search over all possible AP configurations is prohibitively complex. Motivated by this, we formulate the problem of optimally scheduling APs in the UL or DL modes to maximize the sum UL-DL SE in a DTDD enabled CF-mMIMO system and propose a scalable solution by exploiting a sub-modularity property of the sum UL-DL SE.

We note that, in CF-mMIMO systems, a natural UE grouping by the serving BSs does not exist, unlike a cellular mMIMO system. Also, in cellular mMIMO, only the serving BS aims to estimate the channel from a given UE, while in a CF-mMIMO system, all the APs in the vicinity of a given UE need to obtain good channel estimates. Therefore, in order to mitigate pilot contamination, one needs to revisit the problem of pilot allocation across UEs in CF-mMIMO systems. For example, physically proximal UEs should not use the same pilot sequences. Therefore, in this paper, we also address the problem of pilot allocation in CF-mMIMO systems along with the problem of AP-scheduling.

C. Contributions:

In this paper, we investigate how to facilitate DTDD in a CF-mMIMO system with HD-APs. DTDD allows us to partition the time-slots at each AP into UL and DL slots according to the UL and the DL traffic demands at the UEs. The scheduling of APs based on the data demands and analyzing the resulting network throughput performance is the main goal of this work. Our main contributions are as follows:

1) We formulate the AP-scheduling problem as one of maximizing the sum UL-DL SE given the traffic demands from the UEs and considering matched filter precoding (MFP) in the DL and maximal ratio combining (MRC) in the UL based on the locally estimated channels. This problem turns out to be NP-hard, and hence the computational complexity of a brute force search based solution grows exponentially with the number of APs. We first argue that the achievable sum UL-DL SE is a monotonic nondecreasing function of the set of scheduled APs. Then, we observe that the dependence of the sum UL-DL SE on the scheduled AP-set is non-linear in nature and therefore proving sub-modularity becomes mathematically intractable. To circumvent that, we derive the following results:
   a) We lower bound the sum UL-DL SE and prove that problem of maximizing the lower bound is equivalent to the problem of maximizing product of the SINRs.
   b) We prove that product of the SINRs of all UEs is a sub-modular set function of the APs scheduled in the system. (See Theorem 3.)
2) This allows us to develop a greedy algorithm for dynamic AP-scheduling, where, at each step, the transmission mode of the AP that maximizes the incremental SE is added to the already scheduled AP-subset. The lower bound on the sum UL-DL SE achieved by the solution obtained via the greedy algorithm is guaranteed to be within a $(1-\frac{1}{e})$-fraction of its global optimal value. (See Algorithm 1.) We note that the computational complexity of the greedy algorithm is linear in the number of APs.
3) We also analyze the UL and DL SE considering a minimum mean square error (MMSE) based combiner in the UL and regularized zero forcing (RZF) precoder in the DL, and demonstrate the performance improvement obtained compared to MRC and MFP.

4) We then shift focus to the problem of allocating pilot sequences across the UEs. In a CF system, optimal pilot allocation is also a combinatorial optimization problem, and unless the pilots are judiciously assigned across UEs, pilot contamination can lead to poor channel estimates at multiple APs. Therefore, we develop an iterative pilot allocation algorithm based on locally estimated channel statistics (see Algorithm 2) at the APs. This algorithm does not require extra signaling overhead in the form of inter-AP coordination. (See Sec. VII.)

Our experimental results show that the greedy algorithm procures a sum UL-DL SE that matches with exhaustive search based AP-scheduling, and that the algorithm is robust to both inter-UE and inter-AP CLI. Furthermore, DTDD CF-mMIMO substantially enhances the system performance compared to static TDD based CF as well as cellular systems. Interestingly, the DTDD based CF-system outperforms an FD cellular mMIMO system under both MRC & MFP as well as MMSE & RZF combiner and precoder employed at the APs/BSs. For example, a CF-DTDD system with $(M = 16, N = 64)$ even outperforms the cellular FD-system having twice the antenna density, i.e., $(L = 16, N_t = N_r = 64)$. If we increase the number of APs with half the antenna density compared to the FD (see the curve corresponding to $(M = 64, N = 16)$ in Fig. 6a), the sum UL-DL SE offered by HD CF-DTDD improves, significantly outperforming the cellular FD system.

We conclude that, due to the benefits offered by joint signal processing at the CPU, HD CF-mMIMO with dynamic AP-scheduling offers improved sum SE as well as 90%-likely SE compared to static TDD based CF systems and even the cellular FD mMIMO system. Therefore, DTDD enabled CF-mMIMO system with appropriately scheduled APs is a promising solution to meet the heterogeneous traffic loads in next generation wireless systems.

Notations: Matrices, vectors, and sets are denoted by bold upper-case, bold lower-case, and calligraphic letters, respectively. $(\cdot)^T$, $(\cdot)^H$, $(\cdot)^*$, and tr$(\cdot)$ represent transposition, hermitian, complex conjugation, and trace operations, respectively. $|\cdot|$, $\setminus$, $'$, and $\cup$ denote the cardinality, set-subtraction, complement, and union of sets, respectively. $\mathbb{E}[\cdot]$ and $\texttt{var}\{\cdot\}$ denote the mean and variance of a random variable, respectively. $\mathbf{x} \sim \mathcal{CN}(\mathbf{0}, \boldsymbol{\Sigma}_N)$ indicates that $\mathbf{x}$ is a zero mean circularly symmetric complex Gaussian (CSCG) random vector with covariance matrix $\boldsymbol{\Sigma}_N \in \mathbb{C}^{N\times N}$. Other frequently used symbols are cataloged in Table I.

II. System Model and Problem Statement

We consider a CF-mMIMO system with M HD-APs jointly and coherently serving K single-antenna UEs. Each AP is equipped with N antennas and is connected to the CPU via an infinite capacity front-haul link. Time is divided into slots, and in any given slot, each AP can operate either in the UL mode or in the DL mode. We assume that the UL/DL traffic demands of the UEs are known at the CPU; its task is to decide the mode of operation of each AP based on the traffic demands in its vicinity.

The channel from kth UE to the mth AP is modeled as $\mathbf{f}_{mk} = \sqrt{\beta_{mk}}\mathbf{h}_{mk} \in \mathbb{C}^N$, where $\beta_{mk} > 0$ denotes the large scale fading and path loss coefficient, and are known to the APs and the CPU. Note that β_{mk} remains unchanged over several channel coherence intervals [1]–[3]. The fast fading components, $\mathbf{h}_{mk} \sim \mathcal{CN}(\mathbf{0}, \mathbf{I}_N) \in \mathbb{C}^N$, are independent and identically distributed (i.i.d.) and are estimated at the APs (and the CPU) using pilot signals. Under a quasi-static fading model, $\mathbf{h}_{mk}$ remains constant over one coherence interval, and takes independent values from the same distribution in subsequent coherence intervals [1]–[3], [21]–[24]. While the foregoing analysis can be extended to the case of spatially correlated channels with some effort, the equations become cumbersome and do not offer significant additional insights.

Due to simultaneous UL and DL data transmissions, the APs transmitting in the DL cause interference to the APs receiving the UL data, which is the source of inter-AP interference. However, since the channel state information (CSI) of the inter AP channels available at the CPU may be erroneous, residual inter AP interference exists even after interference cancellation. In the literature, the residual interference is modeled as Gaussian distributed additive noise [19], [25]–[28]; we use the same approach. We model the residual interference channel between jth DL AP and the mth UL AP by $\mathbf{G}_{mj} \in \mathbb{C}^{N\times N}$, with its elements being i.i.d. $\mathcal{CN}(0, \zeta_{mj})$, where ζ_{mj} depends on the inter AP path loss and channel estimation error variance. Similarly, we let g_{nk} denote the channel between nth UL UE and the kth DL UE, and we model $\mathrm{g}_{nk} \sim \mathcal{CN}(0, \epsilon_{nk})$ and independent across all UEs [25], [27].

A. Problem Statement

In this work, we investigate DTDD in a CF mMIMO system with HD APs. Let $\mathcal{A}$ be the set of AP indices, with $M = |\mathcal{A}|$. Let the indices of the APs scheduled in the UL and DL modes be contained in the index sets $\mathcal{A}_u$ and $\mathcal{A}_d$, respectively. We aim to maximize the achievable sum UL-DL SE $R_{\text{sum}}(\mathcal{A}_u \cup \mathcal{A}_d)$ over all possible choices of $\mathcal{A}_u$ and $\mathcal{A}_d$ by solving:

$$\begin{aligned} &\max_{\mathcal{A}_u,\mathcal{A}_d} \quad R_{\text{sum}}(\mathcal{A}_u \cup \mathcal{A}_d) \\ &\text{s.t.} \quad \mathcal{A}_u, \mathcal{A}_d \subset \mathcal{A}, \quad \mathcal{A}_u \cap \mathcal{A}_d = \emptyset, \quad \mathcal{A}_u \cup \mathcal{A}_d = \mathcal{A}. \end{aligned} \tag{1}$$

Here, the condition $\mathcal{A}_u \cap \mathcal{A}_d = \emptyset$ arises because of the half-duplex constraint at the APs. Evidently, an exhaustive search can be performed across all 2^M possible configurations, but this becomes computationally expensive as M gets large. We develop a low complexity AP scheduling algorithm in Sec. V.

Another aspect that we address in this work relates to the problem of channel estimation. In CF-mMIMO, all APs are potentially interested in estimating the channel from all UEs, as the signals are jointly processed at the CPU. We consider the reuse of a set of orthonormal pilot sequences across the UEs in order to limit the pilot overhead. However, in this case, it is necessary to assign pilots to UEs such that, at any given AP, the UEs in its vicinity are assigned orthogonal pilots, as far as possible. We address this problem in Sec. VII.

We next discuss the CF-mMIMO signal model within each slot and the channel estimation at the APs, which is our point of departure in this work.

Table I: Symbols

Symbol	Definition	Symbol	Definition
$\mathbf{A} \in \mathbb{C}^{m\times n}$	A matrix with m rows and n columns	$\mathbf{a} \in \{0,1\}^n$	An n length vector with each element being either 0 or 1
$\mathbf{I}_N$	Identity matrix of dimension $N \times N$	$\lvert\mathcal{A}\rvert = n$	$\mathcal{A}$ is an index set with cardinality n
$\mathcal{A}(m)$	mth element of the index set $\mathcal{A}$	$\{\boldsymbol{\phi}_1, \boldsymbol{\phi}_2, \ldots, \boldsymbol{\phi}_{\tau_p}\}$	The set of τ_p orthonormal pilot sequences
$\mathcal{I}_p$	The set of UEs that use the pth pilot sequence	β_{mk}	Pathloss coefficient between the mth AP and kth UE
$\mathbf{h}_{mk}$	Fast fading channel between the mth AP and kth UE	α^2_{mk}	The variance of the kth UE's estimated channel at the mth AP
$\mathcal{E}_{p,k}$	Pilot power of the kth UE	$\mathcal{E}_{u,k}$ and $\mathcal{E}_{d,j}$	UL data power of the kth UE and DL data power of the jth AP
$\mathcal{U}$	Set of all UEs, with $\lvert\mathcal{U}\rvert = K$	$\mathcal{A}$	Set of all AP indices
$\mathcal{U}_u$ and $\mathcal{U}_d$	Set of UL and DL UEs, respectively	κ_{jk}	DL power control coefficient for the kth UE at the jth AP
$\mathcal{A}_u$ and $\mathcal{A}_d$	Set of UL and DL APs, respectively	M and N	Number of APs and antennas per AP, respectively
ϵ_{nk}	The variance of the channel between the nth UL UE and the kth DL UE	ζ_{mj}	The variance of the residual interference channel between the jth DL AP and the mth UL AP

III. Signaling Model and Channel Estimation

We assume that each slot consists of τ symbols or channel uses, of which the first τ_p are used for the UL channel estimation. In these τ_p symbols, all the UEs transmit pilot sequences to the APs. Due to the large number of UEs being served, the training overhead associated with allotting orthogonal pilot sequences to all K UEs could be inordinately high, as it requires $\tau_p \geq K$. Hence, we use a set of τ_p orthonormal pilot sequences denoted by $\{\boldsymbol{\phi}_1, \boldsymbol{\phi}_2, \ldots, \boldsymbol{\phi}_{\tau_p}\}$, where τ_p could be less than K, and $\boldsymbol{\phi}_p \in \mathbb{C}^{\tau_p}, p = 1, \ldots, \tau_p$. These τ_p sequences are allotted to the K UEs, and we denote the indices of the UEs employing the pth pilot sequence by the set $\mathcal{I}_p$. Note that the cardinality of $\mathcal{I}_p$ indicates the repetition factor of the pth pilot sequence, such that $\sum_{p=1}^{\tau_p} |\mathcal{I}_p| = K$. Let $\mathcal{E}_{p,k}$ be the power of the pilot signal by the kth UE. Then, the received pilot signal matrix at the mth AP becomes $\mathbf{Y}_{p,m} = \sum_{p=1}^{\tau_p} \sum_{k\in\mathcal{I}_p} \sqrt{\tau_p \mathcal{E}_{p,k}} \mathbf{f}_{mk} \boldsymbol{\phi}_p^T + \mathbf{W}_{p,m} \in \mathbb{C}^{N\times\tau_p}$, where $\mathbf{W}_{p,m}$ is the receiver noise matrix whose columns are distributed as $\mathcal{CN}(\mathbf{0}, N_0\mathbf{I}_N)$. Post-multiplying $\mathbf{Y}_{p,m}$ by $\boldsymbol{\phi}_p^*$, the processed signal at the mth AP becomes

$$\dot{\mathbf{y}}_{p,m} = \sqrt{\mathcal{E}_{p,k}\tau_p}\mathbf{f}_{mk} + \textstyle\sum_{n\in\mathcal{I}_p\setminus k} \sqrt{\mathcal{E}_{p,n}\tau_p}\mathbf{f}_{mn} + \dot{\mathbf{w}}_{p,m}, \quad (2)$$

with $\dot{\mathbf{w}}_{p,m} = \dot{\mathbf{W}}_{p,m}\boldsymbol{\phi}_p^* \sim \mathcal{CN}(\mathbf{0}, N_0\mathbf{I}_N)$. We can now estimate the channel $\mathbf{f}_{mk}$ using $\dot{\mathbf{y}}_{p,m}$. We have the following result from [29]. The linear minimum mean squared error (LMMSE) estimate of $\mathbf{f}_{mk}$, denoted as $\hat{\mathbf{f}}_{mk}$, can be evaluated as $\hat{\mathbf{f}}_{mk} = \mathbb{E}[\mathbf{f}_{mk}\dot{\mathbf{y}}_{p,m}^H](\mathbb{E}[\dot{\mathbf{y}}_{p,m}\dot{\mathbf{y}}_{p,m}^H])^{-1}\dot{\mathbf{y}}_{p,m}$, which becomes $\hat{\mathbf{f}}_{mk} = \frac{\sqrt{\tau_p\mathcal{E}_{p,k}}\beta_{mk}}{\tau_p\mathcal{E}_{p,k}\beta_{mk} + \tau_p\sum_{n\in\mathcal{I}_p\setminus k}\mathcal{E}_{p,n}\beta_{mn} + N_0}\dot{\mathbf{y}}_{p,m}$, and $\hat{\mathbf{f}}_{mk} \sim \mathcal{CN}(\mathbf{0}, \alpha^2_{mk}\mathbf{I}_N)$, with $\alpha^2_{mk} = c_{mk}\tau_p\mathcal{E}_{p,k}\beta^2_{mk}$, and $c_{mk} \triangleq (\tau_p\mathcal{E}_{p,k}\beta_{mk} + \tau_p\sum_{n\in\mathcal{I}_p\setminus k}\mathcal{E}_{p,n}\beta_{mn} + N_0)^{-1}$. The estimation error, denoted by $\tilde{\mathbf{f}}_{mk} \triangleq \mathbf{f}_{mk} - \hat{\mathbf{f}}_{mk}$, is distributed as $\mathcal{CN}(\mathbf{0}, \bar{\alpha}^2_{mk}\mathbf{I}_N)$, with $\bar{\alpha}_{mk} \triangleq \sqrt{\beta_{mk} - \alpha^2_{mk}}$.

A. Data Transmission

Let $\mathcal{U}_u, \mathcal{U}_d, \mathcal{A}_u$, and $\mathcal{A}_d$ denote the sets containing the indices of UL UEs, DL UEs, UL APs, and DL APs, respectively. Now, let the kth UL UE send the symbol $s_{u,k}$ with power $\mathcal{E}_{u,k}$. The data symbol of each UE is assumed to be zero mean, unit variance, and independent of the data symbols sent by the other UEs. Then, the UL signal received at the mth AP ($m \in \mathcal{A}_u$) can be expressed as

$$\begin{aligned}\mathbf{y}_{u,m} = &\sqrt{\mathcal{E}_{u,k}}\mathbf{f}_{mk}s_{u,k} + \textstyle\sum_{n\in\mathcal{U}_u\setminus k}\sqrt{\mathcal{E}_{u,n}}\mathbf{f}_{mn}s_{u,n} \\ &+ \textstyle\sum_{j\in\mathcal{A}_d}\mathbf{G}_{mj}\mathbf{x}_{d,j} + \mathbf{w}_{u,m} \in \mathbb{C}^N, \end{aligned} \quad (3)$$

where $\mathbf{w}_{u,m} \sim \mathcal{CN}(\mathbf{0}, N_0\mathbf{I}_N)$ is the additive noise, and $\mathbf{x}_{d,j} = \sqrt{\mathcal{E}_{d,j}}\mathbf{P}_j\mathrm{diag}(\boldsymbol{\kappa}_j)\mathbf{s}_d$ is the transmitted DL data vector, with $\mathcal{E}_{d,j}$ being the total power, $\mathbf{P}_j \in \mathbb{C}^{N\times K_d}$ being the precoding matrix, and $\boldsymbol{\kappa}_j$ being the vector of power control coefficients, all at the jth DL AP. Note that κ_{jn}, i.e., the nth element of $\boldsymbol{\kappa}_j$, indicates the fraction of power dedicated by the jth AP to the the nth DL UE ($n \in \mathcal{U}_d$). Typically, κ_{jn} is designed such that $\mathbb{E}\left[\|\mathbf{x}_{d,j}\|^2\right] \leq \mathcal{E}_{d,j} \Rightarrow \sum_{n\in\mathcal{U}_d}\kappa_{jn}\mathbb{E}\|\mathbf{p}_{jn}\|^2 \leq 1$ [1].

Let $\mathbf{v}_{mk}$ denote the locally available combining vector at the mth AP for the kth UE's UL data stream. The kth component of the accumulated signal received at the CPU, $r_{u,k} \triangleq \sum_{m\in\mathcal{A}_u}\mathbf{v}_{mk}^H\mathbf{y}_{u,m}$, can be expanded as

$$\begin{aligned}r_{u,k} = &\textstyle\sum_{m\in\mathcal{A}_u}\sqrt{\mathcal{E}_{u,k}}\mathbf{v}_{mk}^H\mathbf{f}_{mk}s_{u,k} \\ &+ \textstyle\sum_{m\in\mathcal{A}_u}\sum_{n\in\mathcal{U}_u\setminus k}\sqrt{\mathcal{E}_{u,n}}\mathbf{v}_{mk}^H\mathbf{f}_{mn}s_{u,n} \\ &+ \textstyle\sum_{j\in\mathcal{A}_d}\sqrt{\mathcal{E}_{d,j}}\sum_{n\in\mathcal{U}_d}\kappa_{jn}\sum_{m\in\mathcal{A}_u}\mathbf{v}_{mk}^H\mathbf{G}_{mj}\mathbf{p}_{jn}s_{d,n} \\ &+ \textstyle\sum_{m\in\mathcal{A}_u}\mathbf{v}_{mk}^H\mathbf{w}_{u,mk}, \end{aligned} \quad (4)$$

where $\mathbf{p}_{jn}$ is the nth column of $\mathbf{P}_j$. Similarly, assuming perfect channel reciprocity, the signal received by the nth ($n \in \mathcal{U}_d$) DL UE can be expressed as

$$\begin{aligned}r_{d,n} = &\textstyle\sum_{j\in\mathcal{A}_d}\kappa_{jn}\sqrt{\mathcal{E}_{d,j}}\mathbf{f}_{jn}^T\mathbf{p}_{jn}s_{d,n} + \sum_{k\in\mathcal{U}_u}\sqrt{\mathcal{E}_{u,n}}\mathbf{g}_{nk}s_{u,k} \\ &+ \textstyle\sum_{j\in\mathcal{A}_d}\sum_{q\in\mathcal{U}_d\setminus n}\kappa_{jq}\sqrt{\mathcal{E}_{d,j}}\mathbf{f}_{jn}^T\mathbf{p}_{jq}s_{d,q} + w_{d,n}, \end{aligned} \quad (5)$$

where $w_{d,n} \sim \mathcal{CN}(0, N_0)$ is the AWGN at the nth DL UE.

We illustrate the frame structure described above, and contrast it with the frame structure in a TDD based CF system, in Fig. 1. We can now derive the achievable UL and DL SEs for the DTDD enabled CF-mMIMO system.

IV. Spectral Efficiency Analysis: MRC & MFP

In this section, we derive the achievable SEs considering MFP in the DL and MRC in the UL. Here, we first consider MFP and MRC for ease of exposition, and also because it

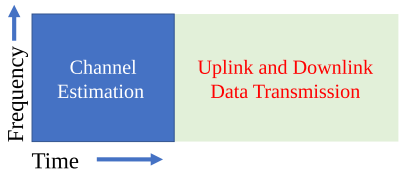

(a) Frame structure of DTDD based CF system

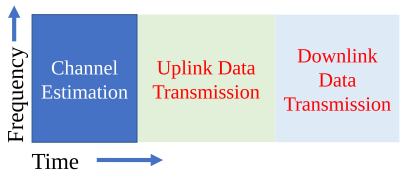

(b) Frame structure of TDD based CF system

Fig. 1. DTDD utilizes same time frequency resources for simultaneous UL and DL data transmission by different HD UEs/APs, unlike TDD, where time is partitioned between the UL and DL UEs.

suffices to elucidate the main point of this work, namely, the benefits obtainable by enabling DTDD in a CF-mMIMO system. In several other works, for example in [1], [30], [31], MRC and MFP have been extensively used for the tractable and interpretable analysis. For deriving the UL and DL SE, we employ the *use-and-then-forget* capacity bounding technique whose effectiveness in CF-mMIMO systems has been well established [1], [3], [30].

Now, with $\mathbf{v}_{mk} = \hat{\mathbf{f}}_{mk}$ in (4), the kth UE's of the combined signal at the CPU becomes

$$\begin{aligned} r_{u,k} &= \sqrt{\mathcal{E}_{u,k}}\mathbb{E}\big[\sum_{m\in\mathcal{A}_u}\hat{\mathbf{f}}_{mk}^H\mathbf{f}_{mk}\big]s_{u,k} \\ &+\sqrt{\mathcal{E}_{u,k}}\big\{\sum_{m\in\mathcal{A}_u}\hat{\mathbf{f}}_{mk}^H\mathbf{f}_{mk} - \mathbb{E}\big[\sum_{m\in\mathcal{A}_u}\hat{\mathbf{f}}_{mk}^H\mathbf{f}_{mk}\big]\big\}s_{u,k} \\ &+\sum_{m\in\mathcal{A}_u}\hat{\mathbf{f}}_{mk}^H\big\{\sum_{n\in\mathcal{I}_p\setminus k}\sqrt{\mathcal{E}_{u,n}}\mathbf{f}_{mn}s_{u,n} + \sum_{q\in\mathcal{U}_u\setminus\mathcal{I}_p}\sqrt{\mathcal{E}_{u,q}}\mathbf{f}_{mq}s_{u,q}\big\} \\ &+\sum_{m\in\mathcal{A}_u}\sum_{j\in\mathcal{A}_d}\sum_{n\in\mathcal{U}_d}\kappa_{jn}\sqrt{\mathcal{E}_{d,j}}\hat{\mathbf{f}}_{mk}^H\mathbf{G}_{mj}\hat{\mathbf{f}}_{jn}^*s_{d,n} + \sum_{m\in\mathcal{A}_u}\hat{\mathbf{f}}_{mk}^H\mathbf{w}_{u,mk}. \end{aligned} \tag{6}$$

The first and second terms of (6) respectively represent the expected effective array gain and UL beamforming uncertainty, and are uncorrelated with each other. Similarly, the first term is uncorrelated with all the other terms of (6). Invoking the worst case noise theorem [32], the effective SINR of the kth UE's data stream, denoted by $\eta_{u,k}$, can be written as

$$\begin{aligned} \eta_{u,k} &= \mathcal{E}_{u,k}\big[\big|\mathbb{E}\big[\sum_{m\in\mathcal{A}_u}\hat{\mathbf{f}}_{mk}^H\mathbf{f}_{mk}\big]\big|^2\big]\times\big(\mathcal{E}_{u,k}\mathtt{var}\big\{\sum_{m\in\mathcal{A}_u}\hat{\mathbf{f}}_{mk}^H\mathbf{f}_{mk}\big\} \\ &+\sum_{n\in\mathcal{I}_p\setminus k}\mathcal{E}_{u,n}\mathbb{E}\big[\big|\sum_{m\in\mathcal{A}_u}\hat{\mathbf{f}}_{mk}^H\mathbf{f}_{mn}\big|^2\big] + \sum_{q\in\mathcal{U}_u\setminus\mathcal{I}_p}\mathcal{E}_{u,n}\mathbb{E}\big[\big|\sum_{m\in\mathcal{A}_u}\hat{\mathbf{f}}_{mk}^H\mathbf{f}_{mq}\big|^2\big] \\ &+\sum_{n\in\mathcal{U}_d}\mathbb{E}\big[\big|\sum_{m\in\mathcal{A}_u}\sum_{j\in\mathcal{A}_u}\sqrt{\mathcal{E}_{d,j}}\kappa_{jn}\hat{\mathbf{f}}_{mk}^H\mathbf{G}_{mj}\hat{\mathbf{f}}_{jn}^*\big|^2\big] \\ &+N_0\sum_{m\in\mathcal{A}_u}\mathbb{E}\big\|\hat{\mathbf{f}}_{mk}^H\big\|^2\big)^{-1}. \end{aligned} \tag{7}$$

We simplify the above expression in the following theorem.

Theorem 1. *The achievable UL SE for the kth UE can be expressed as $\mathcal{R}_{u,k} = \log_2(1+\eta_{u,k})$, where $\eta_{u,k}$ is the UL SINR which is given by*

$$\eta_{u,k} = \frac{N\mathcal{E}_{u,k}\left(\sum_{m\in\mathcal{A}_u}\alpha_{mk}^2\right)^2}{\mathtt{NCoh}_{u,k} + \mathtt{Coh}_{u,k} + \mathtt{IAP}_{u,k} + N_0\sum_{m\in\mathcal{A}_u}\alpha_{mk}^2}, \tag{8}$$

where α_{mk}^2 is as defined after (2), $\mathtt{NCoh}_{u,k}$ represents the non-coherent inter UE interference, $\mathtt{Coh}_{u,k}$ represents the coherent inter UE interference due to pilot contamination, $\mathtt{IAP}_{u,k}$ represents the inter AP interference, and $N_0\sum_{m\in\mathcal{A}_u}\alpha_{mk}^2$ corresponds to the effect of AWGN in the UL. These are expressed as

$$\mathtt{NCoh}_{u,k} = \sum_{n\in\mathcal{U}_u}\mathcal{E}_{u,n}\sum_{m\in\mathcal{A}_u}\alpha_{mk}^2\beta_{mn}, \tag{9a}$$

$$\mathtt{Coh}_{u,k} = N\sum_{n\in\mathcal{I}_p\setminus k}\mathcal{E}_{u,n}\Big(\sum_{m\in\mathcal{A}_u}\alpha_{mk}^2\sqrt{\frac{\mathcal{E}_{p,n}}{\mathcal{E}_{p,k}}}\frac{\beta_{mn}}{\beta_{mk}}\Big)^2, \tag{9b}$$

$$\mathtt{IAP}_{u,k} = N\sum_{m\in\mathcal{A}_u}\sum_{j\in\mathcal{A}_d}\sum_{n\in\mathcal{U}_d}\kappa_{jn}^2\zeta_{mj}\alpha_{mk}^2\alpha_{jn}^2\mathcal{E}_{d,j}. \tag{9c}$$

Proof. See Appendix A. ■

We now consider the DL case. Letting $\mathbf{p}_{jn} = \hat{\mathbf{f}}_{jn}^*$, the signal received by the nth ($n \in \mathcal{U}_d$) DL UE can be expressed as

$$\begin{aligned} r_{d,n} &= \sum_{j\in\mathcal{A}_d}\kappa_{jn}\sqrt{\mathcal{E}_{d,j}}\mathbb{E}\big[\mathbf{f}_{jn}^T\hat{\mathbf{f}}_{jn}^*\big]s_{d,n} \\ &+\sum_{j\in\mathcal{A}_d}\kappa_{jn}\sqrt{\mathcal{E}_{d,j}}\Big\{\mathbf{f}_{jn}^T\hat{\mathbf{f}}_{jn}^* - \mathbb{E}\big[\mathbf{f}_{jn}^T\hat{\mathbf{f}}_{jn}^*\big]\Big\}s_{d,n} \\ &+\sum_{j\in\mathcal{A}_d}\Big\{\sum_{q\in\mathcal{I}_p\setminus n}\sqrt{\mathcal{E}_{d,j}}\kappa_{jq}\mathbf{f}_{jn}^T\hat{\mathbf{f}}_{jq}^*s_{d,q} + \sum_{q\in\mathcal{U}_d\setminus\mathcal{I}_p}\sqrt{\mathcal{E}_{d,j}}\kappa_{jq}\mathbf{f}_{jn}^T\hat{\mathbf{f}}_{jq}^*s_{d,q}\Big\} \\ &+\sum_{k\in\mathcal{U}_u}\sqrt{\mathcal{E}_{u,n}}\mathbf{g}_{nk}s_{u,k} + w_{d,n}. \end{aligned} \tag{10}$$

We present the DL SE in the following theorem.

Theorem 2. *The achievable DL SE for the nth UE can be expressed as $\mathcal{R}_{d,n} = \log_2(1+\eta_{d,n})$, with DL SINR of the nth UE, $\eta_{d,n}$, expressed as*

$$\eta_{d,n} = \frac{N^2\left(\sum_{j\in\mathcal{A}_d}\kappa_{jn}\sqrt{\mathcal{E}_{d,j}}\alpha_{jn}^2\right)^2}{\mathtt{NCoh}_{d,n} + \mathtt{Coh}_{d,n} + \mathtt{IU}_{d,n} + N_0}, \tag{11}$$

where α_{jn}^2 is as defined after (2), $\mathtt{NCoh}_{d,n}$, $\mathtt{Coh}_{d,n}$, and $\mathtt{IU}_{d,n}$ represent the DL non-coherent interference, coherent interference, and the UE to UE CLI, respectively. These are expressed as

$$\mathtt{NCoh}_{d,n} = N\sum_{q\in\mathcal{U}_d}\sum_{j\in\mathcal{A}_d}\mathcal{E}_{d,j}\kappa_{jq}^2\beta_{jn}\alpha_{jq}^2, \tag{12a}$$

$$\mathtt{Coh}_{d,n} = N^2\sum_{q\in\mathcal{I}_p\setminus n}\Big(\sum_{j\in\mathcal{A}_d}\sqrt{\mathcal{E}_{d,j}}\kappa_{jq}\alpha_{jq}^2\sqrt{\frac{\mathcal{E}_{p,n}}{\mathcal{E}_{p,q}}}\frac{\beta_{jn}}{\beta_{jq}}\Big)^2, \tag{12b}$$

$$\mathtt{IU}_{d,n} = \sum_{k\in\mathcal{U}_u}\mathcal{E}_{u,n}\epsilon_{nk}. \tag{12c}$$

Proof. See Appendix B. ■

Now, the overall sum UL-DL SE of the system can be expressed as

$$\mathcal{R}_{\text{sum}} = \frac{\tau-\tau_p}{\tau}\big[\sum_{k\in\mathcal{U}_u}\mathcal{R}_{u,k} + \sum_{n\in\mathcal{U}_d}\mathcal{R}_{d,n}\big]. \tag{13}$$

We note that, from Theorems 1 and 2, the gain and various interference terms involved in $\mathcal{R}_{u,k}$ and $\mathcal{R}_{d,k}$ are dependent on $\mathcal{A}_u$ and $\mathcal{A}_d$. Therefore, we obtain different values of $\mathcal{R}_{\text{sum}}$ for different choices of $\mathcal{A}_u$ and $\mathcal{A}_d$. To characterize this depen-

dence, from this point onward, we write the achievable sum UL-DL SE as $\mathcal{R}_{\text{sum}}(\mathcal{A}_x)$, where $\mathcal{A}_x \triangleq (\mathcal{A}_u, \mathcal{A}_d)$. Note that, as $\mathcal{U}_u$ and $\mathcal{U}_d$ are given, we omit their dependence on $\mathcal{R}_{\text{sum}}$. Now, the brute-force approach of listing out all the $2^{|\mathcal{A}_u \cup \mathcal{A}_d|}$ possible AP schedules and computing their achievable sum UL-DL SE using (13) makes the complexity of finding an optimal AP schedule exponential in the number of APs. We present a low complexity solution in the next section.

V. Sum Rate Optimization

We recall that the problem of finding the optimal AP schedule, namely, determining which APs should operate in the UL and which APs should operate in the DL, based on the local data demands from the UEs, is a combinatorially complex optimization problem. In this section, we circumvent this by developing a greedy AP-scheduling scheme based on sub-modularity. At each step of the procedure, we select which AP to schedule and whether the scheduled AP should operate in the UL or DL mode, such that the incremental gain in $\mathcal{R}_{\text{sum}}$ is maximized. This process is repeated until the last AP is scheduled, thereby solving the problem in polynomial time. Such a greedy approach to SE maximization has been previously proposed in the antenna selection literature, based on the monotonicity of the cost function [33]. However, to provide concrete guarantees on the performance of the greedy search, we need to show that the cost function is a sub-modular set function of the scheduled APs. In this case, the greedy algorithm is guaranteed to yield a solution that achieves at least $(1-1/e)$-fraction of the optimal value of the cost function. For the sake of completeness, we formally define the monotonicity and sub-modularity properties as follows.

Definition 1. *[34] Let $\mathcal{S}$ be a finite set, and let $2^{\mathcal{S}}$ denote its power set. A function $f : 2^{\mathcal{S}} \to \mathbb{R}$, with $f(\emptyset) = 0$, is said to be* ***monotone nondecreasing*** *if for every $\mathcal{A} \subseteq \mathcal{B} \subseteq \mathcal{S}$, $f(\mathcal{A}) \leq f(\mathcal{B})$, and is said to be* ***sub-modular*** *if for every $\{j\} \in \mathcal{S} \backslash \mathcal{B}$, $f(\mathcal{A} \cup \{j\}) - f(\mathcal{A}) \geq f(\mathcal{B} \cup \{j\}) - f(\mathcal{B})$.*

We first focus on the monotonicity of the sum UL-DL SE. Let $\mathcal{A}$ be the indices of the APs in the network, where each AP (i.e., each index) can be scheduled either in the UL or DL. Further, let $\mathcal{A}_s = \mathcal{A}_u \cup \mathcal{A}_d$ denote the index set of the APs that have been previously scheduled, and $\mathcal{A}'_s = \mathcal{A} \backslash \mathcal{A}_s$ be the index set of unscheduled APs. We need to show that adding an element from $\mathcal{A}'_s$ to $\mathcal{A}_s$ does not decrease $\mathcal{R}_{\text{sum}}$. Now, for any AP $m \in \mathcal{A}'_s$, let $\mathcal{A}_t \triangleq \mathcal{A}_s \cup \{m\}$. We note that when the mth AP is added to the set of UL APs, $\mathcal{A}_u$, it does not introduce any new interference, and hence the sum rate can only improve. However, if the mth AP is added to $\mathcal{A}_d$, then it has the option to transmit with zero power. If it chooses to transmit at zero power, it is as if the AP was not added at all, so the sum rate obtained is the same as that obtained without it. However, if the AP optimally chooses a nonzero transmit power in order to maximize the sum rate, the sum rate can be potentially improved. Hence, the sum rate with the new AP added can only be greater than or equal to the sum rate obtained without the AP, and $\mathcal{R}_{\text{sum}}(\mathcal{A}_s) \leq \mathcal{R}_{\text{sum}}(\mathcal{A}_t)$ with $\mathcal{A}_s \subseteq \mathcal{A}_t$. This shows that the sum rate is a monotone nondecreasing set function.

We now focus on the proof of sub-modularity. First, we observe that due to pilot contamination and CLIs, $\mathcal{R}_{\text{sum}}$ is a non-separable function of the scheduled AP sets $\mathcal{A}_u$ and $\mathcal{A}_d$. For example, if the jth AP, $\{j\} \notin \mathcal{A}_u \cup \mathcal{A}_d$, is scheduled in the UL mode, we can write the gain and the coherent interference terms in (8) and (9b) as

$$\Big(\sum_{m \in \mathcal{A}_u \cup \{j\}} \alpha_{mk}^2\Big)^2 = \Big(\sum_{m \in \mathcal{A}_u} \alpha_{mk}^2\Big)^2 + \alpha_{jk}^4 + 2\alpha_{jk}^2 \sum_{m \in \mathcal{A}_u} \alpha_{mk}^2, \tag{14a}$$

$$\begin{aligned} &\textstyle\sum_{n \in \mathcal{I}_p \backslash k} \mathcal{E}_{u,n} \big(\sum_{m \in \mathcal{A}_u \cup \{j\}} \alpha_{mk}^2 \sqrt{\frac{\mathcal{E}_{p,n}}{\mathcal{E}_{p,k}}} \frac{\beta_{mn}}{\beta_{mk}} \big)^2 \\ &= \textstyle\sum_{n \in \mathcal{I}_p \backslash k} \mathcal{E}_{u,n} \big[\big(\sum_{m \in \mathcal{A}_u} \alpha_{mk}^2 \sqrt{\frac{\mathcal{E}_{p,n}}{\mathcal{E}_{p,k}}} \frac{\beta_{mn}}{\beta_{mk}} \big)^2 \\ &+ \alpha_{jk}^4 \frac{\mathcal{E}_{p,n}}{\mathcal{E}_{p,k}} \frac{\beta_{jn}^2}{\beta_{jk}^2} + 2\alpha_{jk}^2 \sqrt{\frac{\mathcal{E}_{p,n}}{\mathcal{E}_{p,k}}} \frac{\beta_{jn}}{\beta_{jk}} \textstyle\sum_{m \in \mathcal{A}_u} \alpha_{mk}^2 \sqrt{\frac{\mathcal{E}_{p,n}}{\mathcal{E}_{p,k}}} \frac{\beta_{mn}}{\beta_{mk}} \big], \end{aligned} \tag{14b}$$

respectively. We note that in (14a) and (14b), the first two terms in the right hand side correspond to the gain and coherent interferences due to set $\mathcal{A}_u$ and scheduled $\{j\}$th UL AP, respectively. However, due to the nonlinearity and the cross terms, the UL SINR is not a separable function of the set of scheduled APs. Thus, $\eta_{u,k}(\mathcal{A}_u \cup \{j\}) \neq \eta_{u,k}(\mathcal{A}_u) + \eta_{u,k}(\{j\})$. Similar observations hold in DL. Furthermore, in our system, the UL SINRs and the DL SINRs are coupled with the DL transmitted signals via the AP-to-AP CLI and UL transmitted signals via UE-to-UE CLI, respectively, which makes the SINRs dependent on the power control coefficients. Therefore, our problem becomes challenging compared to previous works in antenna selection and UE scheduling literature which have considered either linear cost functions with respect to the maximization sets [35] or perfect CSI at the APs [36].

In several studies, the authors rely on approximations such as high SNR [37], or the SE under asymptotic antenna density [35], which lead to tractable analytical expressions. Such approximate cost function based analysis is known as *sub-modular relaxation* [37]. In this work, we note that as the number of antennas at each AP, N, goes to infinity, the non-coherent interferences becomes negligible compared to the gain and coherent interferences as observed in Theorem 1 and Theorem 2. Also, in a CF-system, the CPU can potentially cancel the AP-AP CLI with the global knowledge of the DL data streams. Therefore, to make the analysis tractable, we bound both the UL and DL rates and formulate an equivalent optimization problem based on the product SINR. Note that, as $N \to \infty$, we can show that

$$\begin{aligned} \mathcal{R}_{u,k} &\geq \log_2 \frac{\mathcal{E}_{u,k} (\sum_{m \in \mathcal{A}_u} \alpha_{mk}^2)^2}{\sum\limits_{n \in \mathcal{I}_p \backslash k} \mathcal{E}_{u,n} (\sum\limits_{m \in \mathcal{A}_u} \alpha_{mk}^2 \sqrt{\frac{\mathcal{E}_{p,n}}{\mathcal{E}_{p,k}}} \frac{\beta_{mn}}{\beta_{mk}})^2} \\ &\geq \log_2 \frac{(\sqrt{\mathcal{E}_{u,k}} \sum_{m \in \mathcal{A}_u} \alpha_{mk}^2)^2}{(\sum\limits_{n \in \mathcal{I}_p \backslash k} \sqrt{\mathcal{E}_{u,n}} \sum\limits_{m \in \mathcal{A}_u} \alpha_{mk}^2 \sqrt{\frac{\mathcal{E}_{p,n}}{\mathcal{E}_{p,k}}} \frac{\beta_{mn}}{\beta_{mk}})^2}, \end{aligned} \tag{15}$$

$$\begin{aligned} \mathcal{R}_{d,n} &\geq \log_2 \frac{(\sum_{j \in \mathcal{A}_d} \kappa_{jn} \sqrt{\mathcal{E}_{j,n}} \alpha_{jn}^2)^2}{\sum\limits_{q \in \mathcal{I}_p \backslash n} (\sum\limits_{j \in \mathcal{A}_d} \sqrt{\mathcal{E}_{d,j}} \kappa_{jq} \alpha_{jq}^2 \sqrt{\frac{\mathcal{E}_{p,n}}{\mathcal{E}_{p,q}}} \frac{\beta_{jn}}{\beta_{jq}})^2} \\ &\geq \log_2 \frac{(\sum_{j \in \mathcal{A}_d} \kappa_{jn} \sqrt{\mathcal{E}_{j,n}} \alpha_{jn}^2)^2}{(\sum\limits_{q \in \mathcal{I}_p \backslash n} \sum\limits_{j \in \mathcal{A}_d} \sqrt{\mathcal{E}_{d,j}} \kappa_{jq} \alpha_{jq}^2 \sqrt{\frac{\mathcal{E}_{p,n}}{\mathcal{E}_{p,q}}} \frac{\beta_{jn}}{\beta_{jq}})^2}. \end{aligned} \tag{16}$$

Algorithm 1: Greedy algorithm for AP scheduling

Inputs: $\mathcal{A}$: the set of all AP indices;
Initialize $\mathcal{A}_u = \mathcal{A}_d = \emptyset$, $\mathcal{A}_s = \mathcal{A}_u \cup \mathcal{A}_d$;
while $\mathcal{A}'_s \neq \emptyset$ **do**
  $i_u^\star = \arg\max_{i \in \mathcal{A}'_s} \mathcal{R}'_{\text{sum}}(\mathcal{A}_u \cup \{i\})$;
  $i_d^\star = \arg\max_{i \in \mathcal{A}'_s} \mathcal{R}'_{\text{sum}}(\mathcal{A}_d \cup \{i\})$;
  if $\mathcal{R}'_{sum}(\mathcal{A}_u \cup \{i_u^\star\}) \geq \mathcal{R}'_{sum}(\mathcal{A}_d \cup \{i_d^\star\})$ **then**
    Update $\mathcal{A}_u = \mathcal{A}_u \cup \{i_u^\star\}$;
    else
      Update $\mathcal{A}_d = \mathcal{A}_d \cup \{i_d^\star\}$
    end
  end
  $\mathcal{A}_s = \mathcal{A}_u \cup \mathcal{A}_d$;
end
Return $\mathcal{A}_u$ and $\mathcal{A}_d$;

The latter lower bounds in (15) and (16) follow as we have only added more interference terms in the denominators. Let $\mathcal{R}'_{u,k} = \log_2 \frac{(\sqrt{\mathcal{E}_{u,k}} \sum_{m \in \mathcal{A}_u} \alpha_{mk}^2)^2}{(\sum_{n \in \mathcal{I}_p \setminus k} \sqrt{\mathcal{E}_{u,n}} \sum_{m \in \mathcal{A}_u} \alpha_{mk}^2 \sqrt{\frac{\mathcal{E}_{p,n}}{\mathcal{E}_{p,k}} \frac{\beta_{mn}}{\beta_{mk}}})^2} = 2\log_2 \frac{\sum_{m \in \mathcal{A}_u} \mathtt{G}_{u,mk}}{\sum_{m \in \mathcal{A}_u} \mathtt{I}_{u,mk}}$ and $\mathcal{R}'_{d,n} = \log_2 \frac{(\sum_{j \in \mathcal{A}_d} \kappa_{jn} \sqrt{\mathcal{E}_{j,n}} \alpha_{jn}^2)^2}{(\sum_{q \in \mathcal{I}_p \setminus n} \sum_{j \in \mathcal{A}_d} \sqrt{\mathcal{E}_{d,j}} \kappa_{jq} \alpha_{jq}^2 \sqrt{\frac{\mathcal{E}_{p,n}}{\mathcal{E}_{p,q}} \frac{\beta_{jn}}{\beta_{jq}}})^2} = 2\log_2 \frac{\sum_{j \in \mathcal{A}_d} \mathtt{G}_{d,jn}}{\sum_{j \in \mathcal{A}_d} \mathtt{I}_{d,jn}}$, with the respective terms being defined as $\mathtt{G}_{u,mk} \triangleq \sqrt{\mathcal{E}_{u,k}} \alpha_{mk}^2$, $\mathtt{I}_{u,mk} \triangleq \sum_{n \in \mathcal{I}_p \setminus k} \sqrt{\mathcal{E}_{u,n}} \alpha_{mk}^2 \sqrt{\frac{\mathcal{E}_{p,n}}{\mathcal{E}_{p,k}} \frac{\beta_{mn}}{\beta_{mk}}}$, $\mathtt{G}_{d,jn} \triangleq \kappa_{jn} \sqrt{\mathcal{E}_{j,n}} \alpha_{jn}^2$, and $\mathtt{I}_{d,jn} \triangleq \sum_{q \in \mathcal{I}_p \setminus n} \sqrt{\mathcal{E}_{d,j}} \kappa_{jq} \alpha_{jq}^2 \sqrt{\frac{\mathcal{E}_{p,n}}{\mathcal{E}_{p,q}} \frac{\beta_{jn}}{\beta_{jq}}}$.

Now, given the set of APs $\mathcal{A}_s$, our problem is to optimally decide the partition $\mathcal{A}_u$ and $\mathcal{A}_d$ such that the sum UL-DL SE, i.e. $\mathcal{R}'_{\text{sum}} \triangleq [\sum_{k \in \mathcal{U}_u} \mathcal{R}'_{u,k} + \sum_{n \in \mathcal{U}_d} \mathcal{R}'_{d,n}]$, is maximized. For notational simplicity, we rewrite our problem as follows

$$\max_{\mathcal{A}_s} \mathcal{R}'_{\text{sum}} = \max_{\mathcal{A}_s} \sum_{k=1}^{K} 2\log_2 \frac{\sum_{m \in \mathcal{A}_s} \mathtt{G}_{mk}(\mathcal{A}_s)}{\sum_{m \in \mathcal{A}_s} \mathtt{I}_{mk}(\mathcal{A}_s)} \overset{(a)}{\equiv} \max_{\mathcal{A}_s} \prod_{k=1}^{K} \frac{\sum_{m \in \mathcal{A}_s} \mathtt{G}_{mk}(\mathcal{A}_s)}{\sum_{m \in \mathcal{A}_s} \mathtt{I}_{mk}(\mathcal{A}_s)}, \quad (17)$$

where the kth UE can be either UL or DL and mth AP is either scheduled in UL or in the DL. Here, we explicitly write the gain and interferences as a function of $\mathcal{A}_s$. The equivalence in (a) follows from the monotonicity of $\log_2(.)$.

Theorem 3. *The product SINR,* $f_{mk}(\mathcal{A}_x) = \prod_{k=1}^{K} \frac{\sum_{m \in \mathcal{A}_x} \mathtt{G}_{mk}(\mathcal{A}_x)}{\sum_{m \in \mathcal{A}_x} \mathtt{I}_{mk}(\mathcal{A}_x)}$, *is a sub-modular function of the number of scheduled APs in the system. That is, if* $\mathcal{A}_s$ *and* $\mathcal{A}_t$ *are index sets of active APs, with* $\mathcal{A}_s \subseteq \mathcal{A}_t$, *and if* $\{j\} \notin \mathcal{A}_t$, *then* $f_{mk}(\mathcal{A}_s \cup \{j\}) - f_{mk}(\mathcal{A}_s) \geq f_{mk}(\mathcal{A}_t \cup \{j\}) - f_{mk}(\mathcal{A}_t)$.

Proof. See Appendix C. ■

Now, exploiting the sub-modularity of $\mathcal{R}'_{\text{sum}}$, we can develop a greedy algorithm for scheduling the APs as detailed in Algorithm 1. It follows that $\mathcal{R}'_{\text{sum}}(\dot{\mathcal{A}}) \geq \left(1 - \frac{1}{e}\right) \mathcal{R}'_{\text{sum}}(\mathcal{A}^\star)$, where $\mathcal{A}^\star$ is the index set containing the optimal AP configuration that maximizes the cost function $\mathcal{R}'_{\text{sum}}$, and $\dot{\mathcal{A}}$ denotes the AP configuration returned by Algorithm 1. We validate the effectiveness of the greedy algorithm via numerical simulations in Fig. 2a. The simulation parameters are detailed in Sec. IX. For the brute force based search, we have considered our original cost function $\mathcal{R}_{\text{sum}}$ as expressed in (13) over all possible AP-schedules to find the optimal SE. We also use the AP schedule generated by Algorithm 1 and evaluate $\mathcal{R}_{\text{sum}}$ using (13). We observe that the sum UL-DL SE obtained via exhaustive search over all 2^M UL-DL AP-configurations and considering the effects of CLIs matches closely with that obtained via Algorithm 1 based on sub-modularity of the lower-bounded cost function.

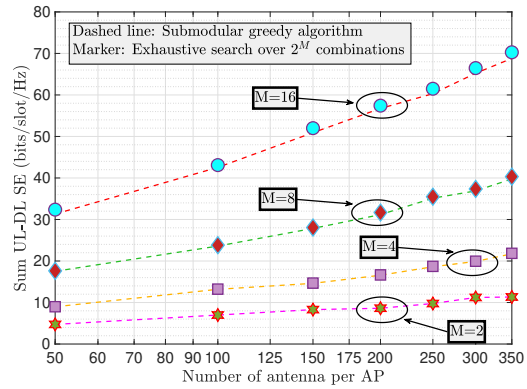

(a) Sum UL-DL SE (bits/slot/Hz) vs number of AP-antennas for different numbers of APs. This plot shows the effectiveness of the sub-modular algorithm.

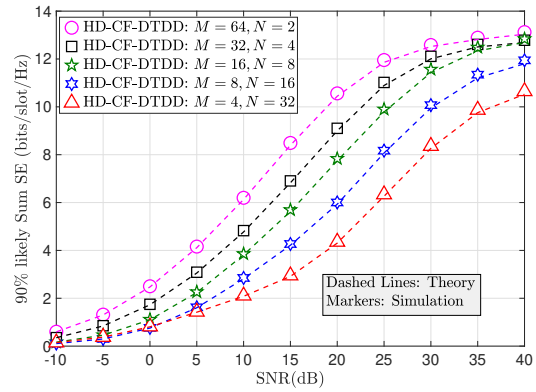

(b) The 90%-likely sum UL-DL SE vs. data SNR with $K = 100$. This figure validates the derived theoretical expressions of the sum SE with Monte Carlo simulations.

Fig. 2. Validation of sum-modular algorithm and the derived expressions of sum UL-DL SE under MRC/MFP.

In Fig. 2b, we plot the 90%-likely sum UL-DL SE vs. UL and DL data SNR to validate the theoretical expressions of SE derived in Theorems 1 and 2. For the simulation, we consider $10,000$ Monte Carlo channel instantiations and UE locations; the other parameters used can be found in Sec. IX. The theoretical curve is obtained by averaging the 90% likely sum SE obtained from (13). The simulation corroborates well with our derived results, verifying the accuracy of the expression for $\mathcal{R}_{\text{sum}}$ derived above.

$$\eta_{u,k} = \frac{\mathcal{E}_{u,k}\left|\hat{\mathbf{f}}_{u,k}^H \mathbf{Q}_u^{-1}\hat{\mathbf{f}}_{u,k}\right|^2}{\sum_{k'\in\mathcal{U}_u\setminus k}\mathcal{E}_{u,k'}\left|\hat{\mathbf{f}}_{u,k}^H \mathbf{Q}_u^{-1}\hat{\mathbf{f}}_{u,k'}\right|^2 + \hat{\mathbf{f}}_{u,k}^H \mathbf{Q}_u^{-1}\left(\mathbf{R}_u + N_0\mathbf{I}_{N|\mathcal{A}_u|}\right)\mathbf{Q}_u^{-1}\hat{\mathbf{f}}_{u,k}}. \tag{20}$$

VI. Performance Analysis: MMSE & RZF

It is known that the performance of CF-mMIMO can be improved with centralized MMSE combining in the UL and RZF precoding in the DL [19], [24]. In this section we briefly analyze the performance of our system model under these combining and precoding schemes.

Let $\mathcal{A}_u(m)$ and $\mathcal{U}_u(k)$ denote the mth UL AP and the kth UL UE in $\mathcal{A}_u$ and $\mathcal{U}_u$, respectively. Let $\mathcal{A}_d(j)$ and $\mathcal{U}_d(n)$ denote the jth DL AP and the nth DL UE in $\mathcal{A}_d$ and $\mathcal{U}_d$, respectively. Let $\hat{\mathbf{f}}_{u,k} \in \mathbb{C}^{N|\mathcal{A}_u|}$ denote the estimated channel matrix of the kth UL UE to all the UL APs, i.e., $\hat{\mathbf{f}}_{u,k} = \left[\hat{\mathbf{f}}_{\mathcal{A}_u(1)k}^T, \ldots, \hat{\mathbf{f}}_{\mathcal{A}_u(|\mathcal{A}_u|)k}^T\right]^T, \forall k \in \mathcal{U}_u$, and let the estimated UL channel matrix available at the CPU be denoted by $\hat{\mathbf{F}}_u \triangleq \left[\hat{\mathbf{f}}_{u,\mathcal{U}_u(1)}, \ldots, \hat{\mathbf{f}}_{u,\mathcal{U}_u(|\mathcal{U}_u|)}\right] \in \mathbb{C}^{N|\mathcal{A}_u|\times|\mathcal{U}_u|}$. Similarly, we can express the estimated channel of the DL UEs as $\hat{\mathbf{F}}_d \triangleq \left[\hat{\mathbf{f}}_{d,\mathcal{U}_d(1)}, \ldots, \hat{\mathbf{f}}_{d,\mathcal{U}_d(|\mathcal{U}_d|)}\right] \in \mathbb{C}^{N|\mathcal{A}_d|\times|\mathcal{U}_d|}$ with $\hat{\mathbf{f}}_{d,n} = \left[\hat{\mathbf{f}}_{\mathcal{A}_d(1)n}^T, \ldots, \hat{\mathbf{f}}_{\mathcal{A}_d(|\mathcal{A}_d|)n}^T\right]^T \in \mathbb{C}^{N|\mathcal{A}_d|}, \forall n \in \mathcal{U}_d$. Now, the concatenated UL signal received at the CPU becomes

$$\mathbf{y}_u = \sum_{k\in\mathcal{U}_u}\sqrt{\mathcal{E}_{u,k}}\left(\hat{\mathbf{f}}_{u,k} + \tilde{\mathbf{f}}_{u,k}\right)s_{u,k} + \sum_{n\in\mathcal{U}_d}\mathbf{G}\mathbf{p}_n s_{d,n} + \mathbf{w}_{ul}, \tag{18}$$

where $\mathbf{G} \in \mathbb{C}^{N|\mathcal{A}_u|\times N|\mathcal{A}_d|}$ denotes the residual interference channel between DL APs and UL APs, and $\mathbf{p}_n \in \mathbb{C}^{N|\mathcal{A}_d|}$ is the nth column of the DL precoder $\mathbf{P} = \left[\mathbf{p}_{\mathcal{U}_d(1)}, \ldots, \mathbf{p}_{\mathcal{U}_d(|\mathcal{U}_d|)}\right] \in \mathbb{C}^{N|\mathcal{A}_d|\times|\mathcal{U}_d|}$. With a slight abuse of notation, let $\mathbf{P}_j \in \mathbb{C}^{N\times|\mathcal{U}_d|}$ denote the precoding matrix for the jth DL AP, and let $\mathcal{E}_{d,j}$ denote the power budget per antenna at the jth DL AP, so that the power constraint becomes $\mathrm{tr}(\mathbf{P}_j\mathbf{P}_j^H) \leq N\mathcal{E}_{d,j}$ [19]. Finally, $\mathbf{w}_{ul} \sim \mathcal{CN}(\mathbf{0}, \mathbf{I}_{N|\mathcal{A}_u|})$ is the additive noise. Then, $\mathbf{V} = \mathbf{Q}_u^{-1}\hat{\mathbf{F}}_u \in \mathbb{C}^{N|\mathcal{A}_u|\times|\mathcal{U}_u|}$ is the joint MMSE combiner, with $\mathbf{Q}_u = \left(\sum_{k\in\mathcal{U}_u}\mathcal{E}_{u,k}\hat{\mathbf{f}}_{u,k}\hat{\mathbf{f}}_{u,k}^H + \mathbf{R}_u + N_0\mathbf{I}_{N|\mathcal{A}_u|}\right)$, where

$$\mathbf{R}_u = \Big(\sum_{k\in\mathcal{U}_u}\mathcal{E}_{u,k}\mathbb{E}\big[\tilde{\mathbf{f}}_{u,k}\tilde{\mathbf{f}}_{u,k}^H\big] + \sum_{i\in\mathcal{U}_d}\mathbb{E}\big[\mathbf{G}\mathbf{p}_n\mathbf{p}_n^H\mathbf{G}^H\big]\Big). \tag{19}$$

Then, the UL sum SE becomes [24] $\mathcal{R}_u = \sum_{k\in\mathcal{U}_u}\mathbb{E}\left[\log_2\left(1+\eta_{u,k}\right)\right]$, where $\eta_{u,k}$ is expressed in (20), with the expectation being taken over the channel realizations. The MMSE combiner presented here maximizes the kth UL UE's instantaneous SINR [24], [32].

In the DL, the RZF precoder is a commonly used linear precoding scheme to control inter-UE interference [19]. It is designed as $\mathbf{P} = \kappa\mathbf{Q}_d^{-1}\hat{\mathbf{F}}_d$, where $\mathbf{Q}_d = \left(\hat{\mathbf{F}}_d\hat{\mathbf{F}}_d^H + \xi\mathbf{I}_{N|\mathcal{A}_d|}\right)$, κ is the power normalization factor, and $\xi > 0$ is a regularization parameter [38], [39]. The DL sum SE can be increased by appropriately selecting ξ [38], and the DL power control parameter κ is evaluated at the CPU based on the estimated channel statistics. Considering an equal power budget at each DL AP, i.e. $\mathcal{E}_{d,j} = \mathcal{E}_d$, it is easy to show $\kappa_j^2 = N\mathcal{E}_d/\mathrm{tr}(\mathbf{P}_j\mathbf{P}_j^H)$ satisfies the DL power constraint. We set $\kappa^2 = \min_j \kappa_j^2$, for all $j \in \mathcal{A}_d$, an approach previously used in [40]. We consider that the DL UEs know the mean of the precoded signal, and therefore, applying the use-and-then forget bound, we can write the DL SE as $\mathcal{R}_d = \sum_{n\in\mathcal{U}_d}\log_2\left(1+\eta_{d,n}\right)$, with $\eta_{d,n}$ (expressed in (21)) being the DL SINR of the nth UE, where the expectations are taken over the channel realizations.

With the above UL and DL SE expressions in hand, we can compare MRC/MFP based combiner/precoding with the MMSE-type combining/precoding. The APs are scheduled according to Algorithm 1, with the sum rate computed using the UL and DL SINRs evaluated according to (20) and (21), respectively. In Fig. 3, we see that, with $(M = 64, N = 4)$, the 90%-sum UL-DL SE achieved via MMSE/RZF is double the sum UL-DL SE achieved via MRC/MFP under similar settings. This shows the interference suppression capability of MMSE-based combiner and precoder, as well as the benefits of the centralized MMSE-processing scheme. However, the complexity of these schemes increase significantly with system dimension, i.e., number of UEs and number of APs. Also, when we increase the number of APs from 8 to 64, we observe a substantial performance improvement irrespective of the processing scheme. There are two contributing factors to this improvement: First, as we increase the number of APs, the flexibility to schedule the APs either in UL or in DL mode also increases, and therefore, the sum UL-DL SE improves considerably. Second, with more APs, the probability that an UE finds an AP (or APs) in its proximity also increases, and which in turn improves the rate achieved by that UE, leading to an improvement in sum UL-DL SE.

VII. Pilot Allocation

The problem of pilot allocation in a CF-mMIMO system is fundamentally different from similar problems encountered in the cellular version. In cellular mMIMO systems, we can avoid intra-cell pilot contamination by allotting orthogonal pilots to all the UEs within each cell [29]. Also, in cellular systems, only the serving BS estimates the channel for each UE. However, in a CF system, it is not just the nearest AP that is interested in estimating the channel of a given UE; all the (nearby) APs need to estimate the channel in order to correctly combine the signals from all the UEs. Moreover, allotting orthogonal pilots to all UEs in the entire geographical zone could lead to a very high pilot overhead as the length of orthogonal pilots scales linearly with the total number of UEs [2], [21]–[23]. On the other hand, reusing a set of orthogonal pilots can result in pilot-sharing UEs in close proximity, leading to high pilot contamination. Hence, there is a need to revisit the problem of pilot allocation across UEs in the context of CF systems.

The authors in [21], [23] present a joint AP-UE clustering based pilot allocation algorithm that maximizes the sum SE. However, we consider the canonical CF-architecture where every UE can potentially be served by all the APs [1], [2],

$$\eta_{d,n} = \frac{\kappa^2 \left|\mathbb{E}\left[\mathbf{f}_n^H \mathbf{Q}_d^{-1} \hat{\mathbf{f}}_n\right]\right|^2}{\kappa^2 \sum_{n' \in \mathcal{U}_d \setminus n} \mathbb{E}\left[\left|\mathbf{f}_n^H \mathbf{Q}_d^{-1} \hat{\mathbf{f}}_{n'}\right|^2\right] + \mathtt{var}\left(\mathbf{f}_n^H \mathbf{Q}_d^{-1} \hat{\mathbf{f}}_n\right) + \sum_{k \in \mathcal{U}_u} \mathcal{E}_{u,k} \mathbb{E}\left|\mathbf{g}_{nk}\right|^2 + N_0} \tag{21}$$

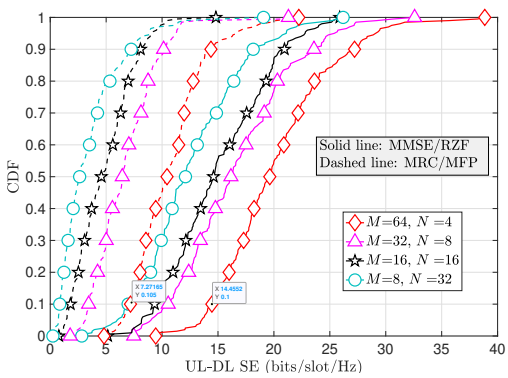

Fig. 3. Performance comparison of MMSE-type precoder/combiner with MRC/MFP with $K = 32$.

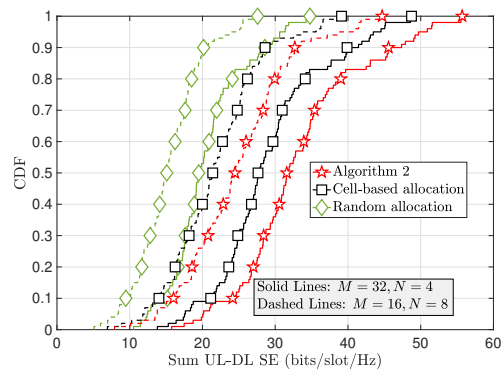

Fig. 4. Cumulative distribution function (CDF) of the achievable sum UL-DL SE under the pilot allocation obtained from Algorithm 2. Here, $K = 100, \tau_p = 25, N_{\text{iter}} = 1000$, and pilot SNR $= 20$ dB.

and hence, the clustering based algorithms cannot be directly applied to our model. In [21], [23], TDD is considered, where, after clustering, all clusters operate either in UL or in DL at a given point in time. However, in a DTDD based system, the randomly distributed UEs have different UL/DL data demands. Due to this, jointly clustering the AP-UEs in DTDD is a more involved problem. The authors in [22] develop a UE-centric dynamic clustering based pilot allocation scheme to maximize the UL SE. The solution requires the knowledge of the SINR at each UE under all possible pilot allocations to obtain the optimal pilot-UE pair, which entails a large overhead when the number of UEs is large. To summarize, the existing approaches to pilot allocation require significant signaling overhead, and also cannot be directly applied to the settings in our problem. The key feature of our pilot allocation strategy is that by employing pilots before the AP scheduling and data transmission phase, we can decouple the problems of pilot allocation and AP-scheduling, in a DTDD based system, which makes our solution attractive for implementation.

We now develop an iterative algorithm to allocate the pilots to different UEs. Recall from Sec. III that a UE with a good channel estimate at the mth AP has a high $\alpha_{mk}^2 = c_{mk}\tau_p \mathcal{E}_{p,k}\beta_{mk}^2$, where c_{mk} accounts for pilot contamination. As the distance between kth and nth $(k, n \in \mathcal{I}_p)$ UEs decreases, the values of α_{mk}^2 and α_{mn}^2 decrease, resulting in worsening of the channel estimates for both UEs. Hence, we first arbitrarily allocate pilots to all the K UEs, and then we find the UE $k^\star$ with the least value of α_{mk} to its nearest AP, that is, $k^\star = \arg\min_k \alpha_{mk}$, where m is the index of the AP closest to UE k. If $\boldsymbol{\phi}_{k^\star}$ is the associated pilot for this UE, we reallocate a new pilot sequence to this UE from $\{\boldsymbol{\phi}_1, \ldots, \boldsymbol{\phi}_K\} \backslash \boldsymbol{\phi}_{k^\star}$ so that $\alpha_{mk^\star}$ is maximized. We repeat this iterative process either up to a predetermined number of iterations, or if no other pilot sequence from $\{\boldsymbol{\phi}_1, \ldots, \boldsymbol{\phi}_K\} \backslash \boldsymbol{\phi}_{k^\star}$ improves $\alpha_{mk^\star}$, or if $\alpha_{mk^\star}$ exceeds a certain threshold for all UEs. The overall recipe is presented in Algorithm 2.

We illustrate the effectiveness of the proposed algorithm in Fig. 4. In the cell-based allocation scheme, since $\tau_p = 25$, we consider 4 equal sized cells in the system, assign each UE to its nearest cell center, allot orthogonal pilots to the UEs within each cell. In case the number of UEs in any cell exceeds the pilot length, we set the pilot length to equal the maximum group size, thus maintaining orthogonality of the pilots within each cell. This reduces pilot contamination within each cluster of UEs, and therefore outperforms random pilot allocation. However, we see that pilot allocation according to Algorithm 2 significantly improves the overall SE compared to both cell-based grouping and random pilot allocation schemes.

Algorithm 2: Iterative Pilot Allocation

Initialize: $\mathcal{I}_p$ for $1 \le p \le \tau_p$, Number of iterations = N_{iter};
Calculate d_{mk} for all $k \in \mathcal{U}$, $m \in \mathcal{A}$;
Define: $m_k^\star = \arg\min_m d_{mk}$;
Calculate $\alpha_{m_k^\star k}$ for all $k \in \mathcal{U}$;
Initialize: $\alpha_q = \max_k \alpha_{m_k^\star k}$;
$\alpha_{\min} = \min_k \alpha_{m_k^\star k}$;
while $(\alpha_{min} < \alpha_o)$ && $(\alpha_{min} < \alpha_q)$ && $(\mathtt{i} \le N_{iter})$ **do**
  $k^\star = \arg\min_k \alpha_{mk}$;
  $\alpha_q = \alpha_{\min}$;
  for $1 \le p \le \tau_p$ **do**
    $\mathcal{I}_p = \mathcal{I}_p \cup \{k^\star\}$;
    $a_p = \alpha_{m_k^\star k}$;
  end
  $p^\star = \arg\max_p a_p$;
  Reallocate k to $\mathcal{I}_{p^\star}$;
  Update: $\alpha_{\min} = \min_k \alpha_{m_k^\star k}$;
  Set: $\mathtt{i} = \mathtt{i} + 1$;
end

VIII. Full-Duplex Multi-cell Systems

In this section, we briefly present the sum UL-DL SE achieved by an FD-enabled multi-cell mMIMO system, based on [25], to enable fair comparison with the DTDD based CF-mMIMO system. We assume that each cell has one FD BS with N_t transmit and N_r receive antennas. To maintain the consistency with our previous analysis, we assume that the total number of UEs across all cells is same as the total number of UEs (K) in the CF system. Let $\mathcal{U}_{l,u}$ and $\mathcal{U}_{l,d}$ denote the index sets of HD UL and DL UEs within the lth cell, such that $\sum_{l=1}^{L}(|\mathcal{U}_{l,u}| + |\mathcal{U}_{l,d}|) = K$. We also assume that each FD BS can perfectly cancel out its self-interference. However, we do not assume any inter-BS cooperation for interference management. Therefore, each BS experiences interference from neighboring cells. Let the UL channel from kth UE of lth cell to the jth BS be denoted by $\mathbf{f}_{u,jlk} = \sqrt{\beta_{jlk}}\mathbf{h}_{u,jlk} \in \mathbb{C}^{N_r \times 1}$, with β_{jlk} being the slow fading component that includes the path loss, and $\mathbf{h}_{u,jlk} \sim \mathcal{CN}(0, \mathbf{I}_{N_r})$ being the fast fading component. Similarly, the DL channel from the jth BS to the nth DL UE of the lth cell can be modeled as $\mathbf{f}_{d,jln} = \sqrt{\beta_{jln}}\mathbf{h}_{d,jln} \in \mathbb{C}^{N_t \times 1}$. The channel matrix from the DL antenna array of the jth BS to the UL antenna array of the lth BS is denoted by $\mathbf{T}_{jl} \in \mathbb{C}^{N_r \times N_t}$, with each element modeled as $\mathcal{CN}(0, \rho_{ij})$. We model the channel between the kth UL UE of the lth cell and the nth DL UE of l'th cell as $\mathrm{g}_{lk,l'n} \sim \mathcal{CN}(0, \epsilon_{lk,l'n})$.In the channel estimation phase, we assume that all the UL and DL UEs synchronously transmit orthogonal pilots for channel estimation [25], [27]. The UL and the DL estimated channels $\hat{\mathbf{f}}_{u,jlk}$ and $\hat{\mathbf{f}}_{d,jlk}$ of $\mathbf{f}_{u,jlk}$ and $\mathbf{f}_{d,jlk}$, respectively, can be expressed as $\mathbf{f}_{x,jlk} = \hat{\mathbf{f}}_{x,jlk} + \tilde{\mathbf{f}}_{x,jlk}$, $x \in u, d$, with $\tilde{\mathbf{f}}_{x,jlk}$ being the estimation error vector, consisting of i.i.d. entries such that $\tilde{\mathbf{f}}_{x,jlk} \sim \mathcal{CN}(0, (\beta_{jlk} - \sigma_{jlk}^2)\mathbf{I})$ with $\sigma_{jlk} = \sqrt{\frac{\tau_p \mathcal{E}_{p,lk}\beta_{jlk}^2}{\tau_p \sum_{l'} \tau_p \mathcal{E}_{p,l'k}\beta_{jl'k} + N_0}}$. Here, the UEs are numbered such that identically indexed UEs across different cells share the same pilot sequence.

Following this, the UEs and the BSs simultaneously transmit their data. Let $\hat{\mathbf{v}}_{u,jk} \in \mathbb{C}^N$ be the UL combiner kth column of the UL combiner vector designed at the jth BS. Similarly, let $\hat{\mathbf{v}}_{d,jn} \in \mathbb{C}^N$ be the DL precoder designed at the jth BS and is intended for the nth DL UE. Let the kth UL UE of the jth cell transmit its symbol $s_{u,jk}$ with power $\mathcal{E}_{u,jk}$, and the jth BS transmit the precoded DL data $\mathbf{v}_{d,jn}s_{u,jn}$. The total power expended by the jth BS is denoted by $\mathcal{E}_{d,j}$ and the power control coefficient for the corresponding nth UE is denoted by κ_{jn}. We present the sum UL-DL SE for a cellular FD-mMIMO system with MRC (i.e. $\mathbf{v}_{u,lk} = \hat{\mathbf{f}}_{u,llk}$) in the UL and MFP (i.e. $\mathbf{v}_{d,ln} = \hat{\mathbf{f}}_{d,lln}^*$) in the DL in the following Lemma based on [25]:

Lemma 4. *The achievable sum UL-DL SE of a cellular FD-mMIMO system with MRC/MFP is*

$$\mathcal{R}_{sum}^{FD} = \frac{\tau - \tau_p}{\tau} \sum_{l=1}^{L} \Bigg\{ \sum_{k \in \mathcal{U}_u} \log_2(1 + \eta_{u,lk}^{FD}) + \sum_{n \in \mathcal{U}_d} \log_2(1 + \eta_{d,ln}^{FD}) \Bigg\}, \tag{22}$$

with the UL and DL SINRs being $\eta_{u,lk}^{FD} = \frac{N_r \sigma_{llk}^2 \mathcal{E}_{u,lk}}{\mathtt{IBS}_{jk} + \mathtt{MUI}_{u,jk} + N_0}$, *and* $\eta_{d,ln}^{FD} = \frac{N_t^2 \kappa_{ln}^2 \mathcal{E}_{d,l} \sigma_{lln}^4}{\mathtt{IUI}_{ln} + \mathtt{MUI}_{d,ln} + N_0}$, *respectively, with* $\mathtt{IBS}_{jk} \triangleq N_t \sum_{j=1, j \neq l}^{L} \sum_{n \in \mathcal{U}_{j,d}} \kappa_{jn}^2 \mathcal{E}_{d,j} \rho_{lj}$, $\mathtt{MUI}_{u,jk} \triangleq N_r \sum_{j=1, j \neq l}^{L} \sigma_{ljk}^2 \mathcal{E}_{u,jk} + \sum_{j=1}^{L} \sum_{k' \in \mathcal{U}_{j,u}} \beta_{ljk'} \mathcal{E}_{u,jk'}$, $\mathtt{IUI}_{ln} \triangleq \sum_{j=1}^{L} \sum_{k' \in \mathcal{U}_{j,u}} \mathcal{E}_{u,lk'} \epsilon_{jk',ln}$, *and* $\mathtt{MUI}_{d,ln} \triangleq N_t^2 \sum_{j=1, j \neq l}^{L} \sigma_{jln}^2 \sigma_{lln}^2 \mathcal{E}_{d,j} \kappa_{jn}^2 + N_t \sum_{j=1}^{L} \sum_{k' \in \mathcal{U}_{j,d}} \beta_{jln} \sigma_{jjk'}^2 \mathcal{E}_{d,j} \kappa_{jk'}^2$.

IX. Numerical Results

In this section, present numerical insights into the performance of DTDD enabled HD-CF mMIMO systems. The UEs are dropped uniformly at random locations over a 1 km $\times$ 1 km area and are served by M HD-APs, depending on the AP-schedules obtained via Algorithm 1. The APs are arranged in a grid for fair comparison and maximal coverage [3], [24]. The pathloss exponent and the reference distance from each AP are assumed to be -3.76 and 10 m, respectively [1]. The UL SNR is set by fixing the noise variance N_0 to unity and varying the UL powers $\mathcal{E}_{u,k}$ such that $\mathcal{E}_{u,k}/N_0$ equals the desired value. In the DL, we set $\kappa_{jn} = (N \sum_{k' \in \mathcal{U}_d} \alpha_{jk'}^2)^{-1}$ in (10), as in [1], [2]. For the cellular system, we partition the area into L equal sized cells with an FD-mMIMO BS deployed at each of the cell centers, and each UE is served by its nearest BS. The results are obtained by averaging over 10^4 random UE location and channel instantiations.

A. Performance comparison with MRC & MFP:

In Fig. 5, we compare the performance of DTDD CF-mMIMO with TDD based HD cellular and CF mMIMO, via the CDFs of the sum UL-DL SE. We consider $K = 32$ UEs with 50% of the UEs having UL data demand in each time slot. For each instantiation of UE positions, the APs are scheduled using the proposed greedy algorithm. In the cellular case, we consider $L = 8$, with the BS in each cell equipped with N antennas. For the HD TDD-CF and DTDD enabled CF, we consider multiple combinations M and N. From Fig. 5a, we see that DTDD enabled CF-mMIMO system considerably improves the sum UL-DL SE compared to the other schemes. For example, CF-DTDD with $(M = 64, N = 4)$ offers a median sum UL-DL SE of 17 bits/slot/Hz, whereas TDD CF offers only 7 bits/slot/Hz. Next, in Fig. 5b, we compare DTDD CF-mMIMO with cellular TDD mMIMO. Cellular TDD with $(L = 8, N = 256)$ performs similar to DTDD CF-mMIMO with $(M = 16, N = 16)$; note that the antenna density in the cellular system is 8 times the antenna density of the CF system. DTDD schedules the APs based on the localized traffic demand and the UL-DL transmissions occur simultaneously, which results in the dramatic improvement in the system sum UL-DL SE compared to the cellular TDD case.

Next, in Fig. 6a, we compare DTDD CF-mMIMO with an FD cellular system. CF-DTDD with HD APs and $(M = 16, N = 64)$ outperforms the cellular FD-system with double the antenna density, i.e., $(L = 16, N_t = N_r = 64)$. Increasing the number of APs, but still with half the antenna

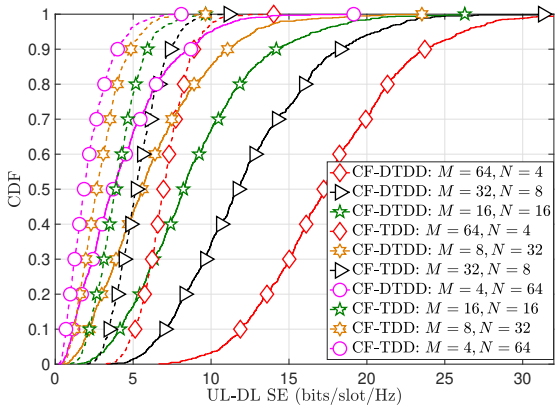

(a) CDF of the sum UL-DL SE of DTDD CF-mMIMO and TDD CF-mMIMO with different AP/antenna configurations.

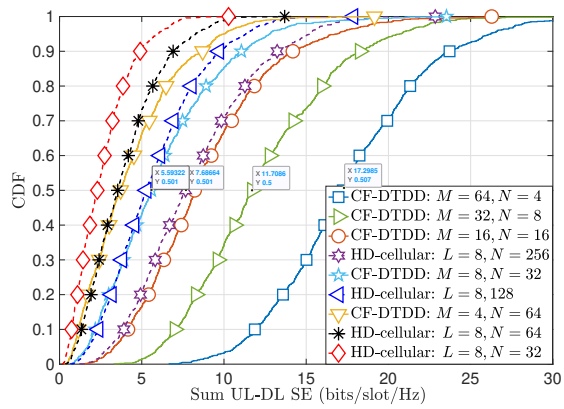

(b) CDF of the sum UL-DL SE of DTDD CF-mMIMO and TDD enabled cellular mMIMO.

Fig. 5. Comparison of DTDD CF-mMIMO with TDD based CF and cellular mMIMO, with MRC/MFP employed at each of the APs/BSs.

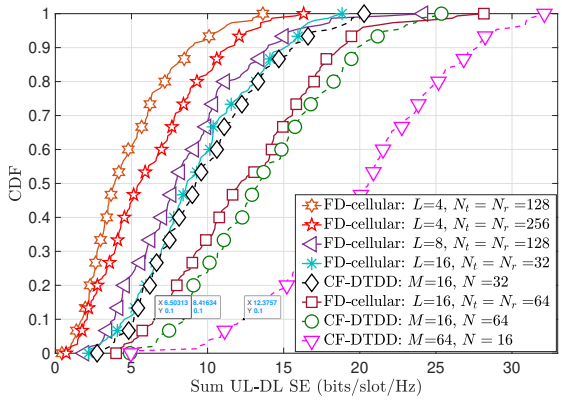

(a) CDF of the sum UL-DL SE of a DTDD CF-mMIMO and a cellular FD-mMIMO system with $K = 32$ UEs.

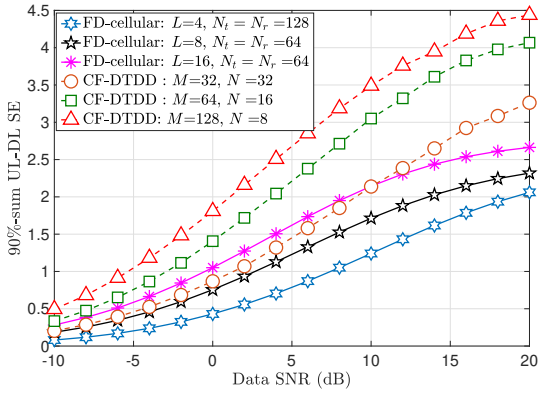

(b) 90%-likely sum UL-DL SE vs. UL and DL data SNR, with $K = 60$ UEs.

Fig. 6. Comparison of DTDD CF-mMIMO with an FD-cellular system.

density compared to the FD (see the curve corresponding to $(M = 64, N = 16)$), results in significantly better sum UL-DL SE in HD CF-DTDD compared to the cellular FD system. Thus, although each BS in cellular system is equipped with simultaneous transmit and receive capability, the HD-APs with dynamic scheduling and the joint processing benefits of DTDD CF-mMIMO results in better sum UL-DL SE.

Next, we illustrate the dependence of the sum UL-DL SE on the data SNR. In Fig. 6b, we plot the average 90%-likely sum UL-DL SE as a function of the UL and DL data SNR. We observe that at low data SNR regime (-10 to 10 dB) an FD-cellular system with $(L = 16, N_t = N_r = 64)$ offers similar 90%-likely UL-DL SE compared to the CF-DTDD system with half the antenna density $(M = 32, N = 32)$. Moreover, if we increase the number of APs deployed, for example $(M = 64, N = 16), (M = 128, N = 8)$, CF-DTDD offers better performance throughout the entire range of data SNR. In both the cases, for a given antenna density, having a larger number of BS/APs is better: the beamforming gains are insufficient to offset the path loss and interference.

In Fig. 7, we show the trade-off between the pilot length and the available data duration via plotting the 90%-likely sum UL-DL SE as a function of the ratio of the number of active UEs to the coherence interval. We consider two cases: (i) $\tau_p = 30$ irrespective of the number of UEs in the system (Fig. 7a), (ii) $\tau_p = K$, i.e., the pilot length is scaled linearly with the UE load (Fig. 7b). We consider the overall fractional UL-DL data demands to be the same across the number of UEs. In case (i), the sum UL-DL SE increases monotonically, even though there is pilot contamination in the system. This shows the effectiveness of the iterative pilot allocation algorithm presented in Sec. VII. However, in case (ii), the duration available for data transmission reduces, leading to a decrease in the SE as the number of UEs increases. For instance, in Fig. 7b, with $(M = 64, N = 2)$, the sum UL-DL SE decreases sharply when UE load goes beyond 55% of the coherence interval. Thus, as the UE load increases, it is better to repeat shorter length pilots, along with a suitable algorithm to ensure minimal pilot contamination, to balance the errors introduced by pilot contamination with the data transmission duration.

Next in Fig. 8a, we investigate the effect of AP-AP and inter-BS CLI on the UL sum SE in CF and cellular mMIMO systems, respectively. Here, we fix the DL SNR to 10 dB for all UEs. We observe that in a cellular FD system, the UL sum SE reduces dramatically when the inter-BS CLI exceeds -40 dB. In contrast, in the DTDD enabled HD CF-mMIMO system, as the AP-AP CLI increases, the greedy algorithm ensures an AP-schedule that balances the UL and DL SE to maximize the

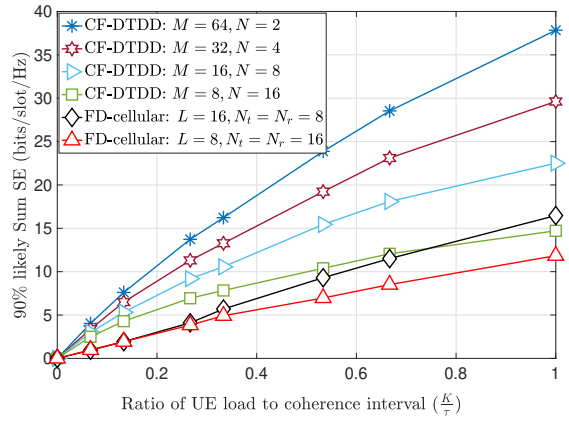

(a) The 90%-likely sum UL-DL SE vs. the number of UEs, with $\tau_p = 30$, $\tau = 200$.

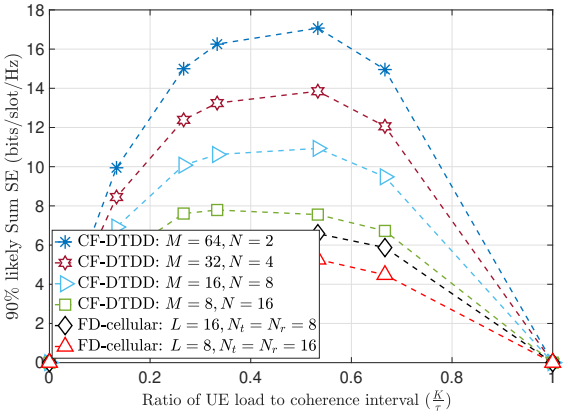

(b) The 90%-likely sum UL-DL SE vs. the number of UEs, with $\tau_p = K$, $\tau = 200$.

Fig. 7. The 90%-likely sum UL-DL SE vs. the number of active UEs. We see that scaling the pilot length with the number of UEs can be detrimental at high UE load; necessitating careful pilot allocation with limited length.

overall sum SE. For instance, with $(M = 32, N = 4)$, as CLI increases from -70 dB to -60 dB, we observe a decrease in the UL SE, and beyond -20 dB, it saturates to about 5 bits/slot/Hz. In contrast, in an FD cellular system with $(L = 8, N_t = N_r = 16)$ the UL SE reduces to nearly 0 bits/slot/Hz at -20 dB of inter-BS CLI. Thus, HD-APs with DTDD are more resilient to SI cancellation errors. Also, the performance of the cellular FD-mMIMO in Fig. 8a is an upper bound, since we consider perfect SI cancelation at the BSs.

In Fig. 8b, to illustrate the effect of the traffic demand on the UL and DL SE, we vary the fraction of UEs demanding UL data from 0 to 1, and plot the 90%-likely UL sum SE against the 90%-likely DL sum SE obtained for each fractional UL-data demand. At each fractional UL-data demand, we use Algorithm 1 to determine the mode of operation across the APs. We observe that the rate region attained by HD CF-DTDD is significantly larger than that of the cellular FD system, e.g., the HD CF-DTDD curve with $(M = 16, N = 8)$ and the FD-cellular curve with $(L = 16, N_t = N_r = 8)$. In fact, even with 100% UL data demand (the points along the x-axis) or 100% DL data demand (the points on the y-axis), HD CF-DTDD outperforms FD-cellular by more than 2 bits/slot/Hz. This is because the FD-cellular system has to contend with inter-cell interference, even if the SI cancelation is perfect. The joint data processing at the CPU and dynamic AP-scheduling based on the UE data demands results in the larger rate region of the HD CF-DTDD mMIMO system.

B. Performance comparison with MMSE & RZF:

In Fig. 9a, we compare the TDD based canonical CF-mMIMO system with our proposed DTDD enabled CF-mMIMO system. For both the schemes, we consider a centralized MMSE combiner in the UL and RZF in the DL. DTDD CF-mMIMO with $(M = 64, N = 2)$ procures a sum UL-DL SE of 14.63 bits/slot/Hz, while in similar settings, the TDD based CF-system only obtains 9.83 bits/slot/Hz. Thus, although MMSE-type combiners and precoders improve the SE of both TDD and DTDD based system, the simultaneous UL-DL data traffic handling capabilities of DTDD based system help further enhance the achievable sum UL-DL SE.

Next, we compare the performance of an FD-enabled cellular mMIMO system with the CF-DTDD based system. For the cellular case, we consider the multi-cell MMSE (M-MMSE) combiner and precoder [32]. From Fig 9b, we observe that an FD cellular system with $(L = 16, N_t = N_r = 32)$ and a CF-DTDD system with $(M = 16, N = 32)$ have a similar CDF of the sum UL-DL SE, in spite of the CF-system having half the antenna density as the FD system. Also, in the CF system, since the APs are HD, only a subset of the 16 APs serve the UL UEs and its complement serves the DL APs. In contrast, all the 16 FD BS can simultaneously serve both UL and DL UEs in their respective cells. We further see that an FD-system with 4 BSs having 128 transmit and receive antennas each offers a 90% sum UL-DL SE of 13.2 bits/slot/Hz, whereas the CF-DTDD based system with $(M = 64, N = 8)$ offers 27 bits/slot/Hz, a more than 100% improvement. Although both FD cellular and CF-DTDD system support simultaneous UL and DL traffic load, the joint signal processing capability at the CPU in the CF architecture helps to substantially improve the sum UL-DL SE.

X. Conclusions

In this paper, we analyzed the performance of an CF-mMIMO system under DTDD where the transmission mode at each HD AP is scheduled so that the sum UL-DL SE is maximized. The complexity of the brute-force search increases exponentially with the number of APs. To tackle this problem, we developed a sub-modularity based greedy algorithm with associated optimality guarantees. Our numerical experiments revealed that a DTDD enabled CF-mMIMO system substantially improves the sum UL-DL SE compared to HD TDD CF and HD TDD cellular mMIMO system. The key reason of the performance improvement in DTDD compared to TDD based systems is that the former duplexing scheme can simultaneously serve the UL and the DL UEs in the system. Furthermore, the HD DTDD CF-mMIMO can even outperform an FD-cellular mMIMO system. Through extensive experiments, we illustrated the sum SE improvement of DTDD CF-mMIMO over the cellular FD system under different antenna densities,

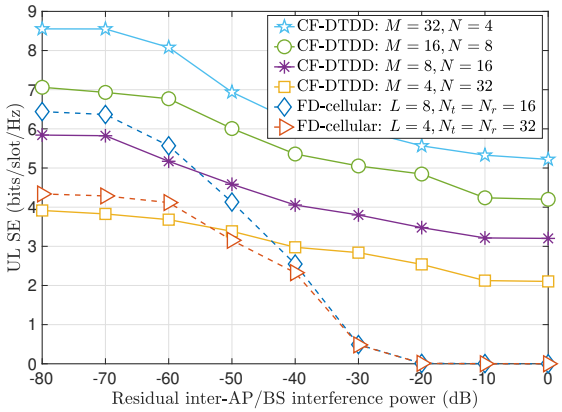

(a) The average UL sum SE vs residual BS-BS/AP-AP cross link interference power. CF-mMIMO system with HD APs and DTDD is more resilient to CLI.

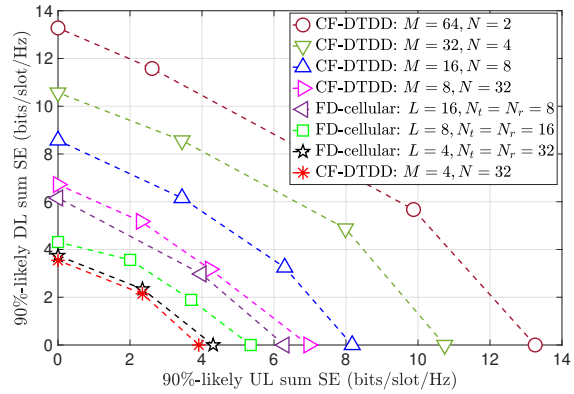

(b) Rate region between 90%-likely UL sum SE vs. 90%-likely DL sum SE. We observe that more APs with smaller antennas provides larger rate region compared to cellular FD system.

Fig. 8. Effect of SI on the UL SE and illustration of rate region under DTDD based CF-mMIMO system.

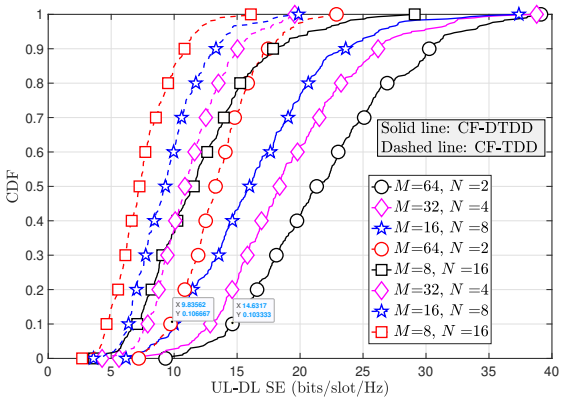

(a) Comparison of DTDD CF-mMIMO and TDD based CF-mMIMO.

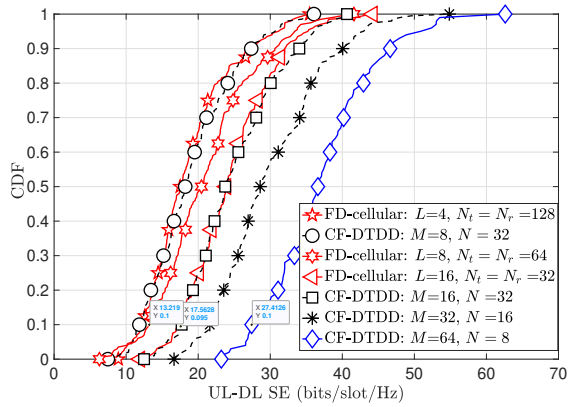

(b) CDF of the sum UL-DL SE achieved via DTDD CF-MIMO and FD mMIMO systems.

Fig. 9. Comparison of DTDD CF-mMIMO with CF-TDD and an FD cellular mMIMO systems.

number of UEs, and fractional UL/DL data demands. We considered the MRC/MFP based scheme as well as the centralized MMSE/RZF based scheme, and in both cellular and CF systems. Under all these different system settings, we showed that CF-DTDD with a large number of APs can improve the sum UL-DL SE compared to an FD cellular system under similar antenna densities. Essentially, DTDD CF-mMIMO exploits the joint signal processing of a CF system coupled with the adaptive scheduling of UL-DL slots based on the localized traffic demands at the APs. We also presented an iterative pilot allocation algorithm which substantially reduces the effect of pilot contamination. A key advantage of DTDD enabled CF over the FD cellular system is that we no longer need additional hardware at each AP to cancel the SI. The system performance can be further improved by incorporating UL-to-DL UE interference cancellation techniques or power control strategies. Another aspect that is worth investigating further is a theoretical analysis of the latency performance of DTDD enabled CF-mMIMO systems, and weighted sum SE maximization with UL/DL fairness constraints. As a final note, an FD-enabled CF-mMIMO system can potentially outperform the HD DTDD CF system, at the cost of SI cancelation hardware at the APs. It would be interesting to theoretically analyze their performance.

Appendix A: Proof of Theorem 1

Proof. The numerator of (6) can be written as $\mathbb{E}[\sum_{m\in\mathcal{A}_u}\hat{\mathbf{f}}_{mk}^H\hat{\mathbf{f}}_{mk}+\hat{\mathbf{f}}_{mk}^H\tilde{\mathbf{f}}_{mk}] = \sum_{m\in\mathcal{A}_u}\mathbb{E}[\|\hat{\mathbf{f}}_{mk}\|^2] = N\sum_{m\in\mathcal{A}_u}\alpha_{mk}^2$. Next, we can show $\mathtt{var}[\sum_{m\in\mathcal{A}_u}\hat{\mathbf{f}}_{mk}^H\mathbf{f}_{mk}] = \sum_{m\in\mathcal{A}_u}N\alpha_{mk}^2\beta_{mk}$. Now, for the UEs that share their pilot sequences with the kth UE, i.e., for $n\in\mathcal{I}_p\backslash k$,

$$\mathbb{E}\Big[\Big|\sum_{m\in\mathcal{A}_u}\hat{\mathbf{f}}_{mk}^H\mathbf{f}_{mn}\Big|^2\Big] = \mathbb{E}\Big[\Big|\sum_{m\in\mathcal{A}_u}c_{mk}\sqrt{\tau_p\mathcal{E}_{p,k}}\beta_{mk} \times\Big(\sum_{n'\in\mathcal{I}_p}\sqrt{\mathcal{E}_{p,n'}\tau_p}\mathbf{f}_{mn'}+\dot{\mathbf{w}}_{p,m}\Big)^H\mathbf{f}_{mn}\Big|^2\Big]$$
$$= N\sum_{m\in\mathcal{A}_u}N_0c_{mk}^2\tau_p\mathcal{E}_{p,k}\beta_{mk}^2\beta_{mn}$$
$$+\mathbb{E}\Big[\Big|\sum_{m\in\mathcal{A}_u}c_{mk}\sqrt{\tau_p\mathcal{E}_{p,k}}\beta_{mk}\sum_{n'\in\mathcal{I}_p}\sqrt{\mathcal{E}_{p,n'}\tau_p}\mathbf{f}_{mn'}^H\mathbf{f}_{mn}\Big|^2\Big]. \quad (23)$$

The last term in the above can be simplified as follows:

$$\mathbb{E}\Big[\Big|\sum_{m\in\mathcal{A}_u}c_{mk}\sqrt{\tau_p\mathcal{E}_{p,k}}\beta_{mk}\Big(\sum_{n'\in\mathcal{I}_p\backslash n}\sqrt{\mathcal{E}_{p,n'}\tau_p}\mathbf{f}_{mn'}$$

$$+\sqrt{\mathcal{E}_{p,n}\tau_p}\mathbf{f}_{mn}\big)^H\mathbf{f}_{mn}\big|^2\big]$$
$$= N\sum_{m\in\mathcal{A}_u} c_{mk}^2\tau_p^2\mathcal{E}_{p,k}\beta_{mk}^2\mathcal{E}_{p,n}\beta_{mn}^2 + N^2\big(\sum_{m\in\mathcal{A}_u}\alpha_{mk}^2\tfrac{\beta_{mn}}{\beta_{mk}}\sqrt{\tfrac{\mathcal{E}_{p,n}}{\mathcal{E}_{p,k}}}\big)^2$$
$$+N\sum_{m\in\mathcal{A}_u}\sum_{n'\in\mathcal{I}_p\backslash n} c_{mk}^2\tau_p^2\mathcal{E}_{p,k}\beta_{mk}^2\mathcal{E}_{p,n'}\beta_{mn'}\beta_{mn}.$$

Now $N\sum_{m\in\mathcal{A}_u}\sum_{n'\in\mathcal{I}_p\backslash n} c_{mk}^2\tau_p^2\mathcal{E}_{p,k}\beta_{mk}^2\mathcal{E}_{p,n'}\beta_{mn'}\beta_{mn}$, can be further expanded as

$$N\sum_{m\in\mathcal{A}_u} c_{mk}\sqrt{\tau_p\mathcal{E}_{p,k}}\beta_{mk}\beta_{mn}\big\{c_{mk}\sqrt{\tau_p\mathcal{E}_{p,k}}\beta_{mk}$$
$$\times\sum_{n'\in\mathcal{I}_p}\tau_p\mathcal{E}_{p,n'}\beta_{mn'}\big\} - N\sum_{m\in\mathcal{A}_u} c_{mk}^2\tau_p^2\mathcal{E}_{p,k}\beta_{mk}^2\mathcal{E}_{p,n}\beta_{mn}^2$$
$$= N\sum_{m\in\mathcal{A}_u}\tau_p\mathcal{E}_{p,k}c_{mk}\beta_{mk}^2\beta_{mn} - NN_0\sum_{m\in\mathcal{A}_u} c_{mk}^2\tau_p\mathcal{E}_{p,k}\beta_{mk}^2\beta_{mn}$$
$$-N\sum_{m\in\mathcal{A}_u} c_{mk}^2\tau_p^2\mathcal{E}_{p,k}\beta_{mk}^2\mathcal{E}_{p,n}\beta_{mn}^2, \tag{24}$$

where, in the last step above, we used the fact $c_{mk}\sqrt{\tau_p\mathcal{E}_{p,k}}\beta_{mk}\sum_{n'\in\mathcal{I}_p}\tau_p\mathcal{E}_{p,n'}\beta_{mn'} = \sqrt{\tau_p\mathcal{E}_{p,k}}\beta_{mk} - N_0c_{mk}\sqrt{\tau_p\mathcal{E}_{p,k}}\beta_{mk}$. Combining (23) and (24), with $\alpha_{mk}^2 = \tau_p\mathcal{E}_{p,k}c_{mk}\beta_{mk}^2$, we obtain

$$\sum_{n\in\mathcal{I}_p\backslash k}\mathcal{E}_{u,n}\mathbb{E}\big[\big|\sum_{m\in\mathcal{A}_u}\hat{\mathbf{f}}_{mk}^H\mathbf{f}_{mn}\big|^2\big]$$
$$=\sum_{n\in\mathcal{I}_p\backslash k}\mathcal{E}_{u,n}\big(N^2\big(\sum_{m\in\mathcal{A}_u}\alpha_{mk}^2\tfrac{\beta_{mn}}{\beta_{mk}}\sqrt{\tfrac{\mathcal{E}_{p,n}}{\mathcal{E}_{p,k}}}\big)^2 + N\sum_{m\in\mathcal{A}_u}\alpha_{mk}^2\beta_{mn}\big). \tag{25}$$

The first two terms above correspond to coherent interference (9b) and non-coherent interference, respectively, from UEs that share the kth UE's pilot. Next, considering the interference due to the UEs that do not share the kth UE's pilot, we obtain

$$\sum_{q\in\mathcal{U}_u\backslash\mathcal{I}_p}\mathcal{E}_{u,n}\mathbb{E}\big[\big|\sum_{m\in\mathcal{A}_u}\hat{\mathbf{f}}_{mk}^H\mathbf{f}_{mq}\big|^2\big]$$
$$= N\sum_{q\in\mathcal{U}_u\backslash\mathcal{I}_p}\mathcal{E}_{u,n}\sum_{m\in\mathcal{A}_u}\tau_p\mathcal{E}_{p,k}c_{mk}\beta_{mk}^2\beta_{mq}. \tag{26}$$

Hence, (9a) follows via combining the beamforming uncertainty, the second term of (25), and (26). Finally, we can derive the inter-AP interference as

$$\sum_{n\in\mathcal{U}_d}\mathbb{E}\big[\big|\sum_{m\in\mathcal{A}_u}\sum_{j\in\mathcal{A}_d}\sqrt{\mathcal{E}_{d,j}}\kappa_{jn}\hat{\mathbf{f}}_{mk}^H\mathbf{G}_{mj}\hat{\mathbf{f}}_{jn}^*\big|^2\big]$$
$$=\sum_{n\in\mathcal{U}_d}\sum_{m\in\mathcal{A}_u}\sum_{j\in\mathcal{A}_d}\mathcal{E}_{d,j}\kappa_{jn}^2\mathbb{E}\big[\mathrm{tr}\big(\mathbf{G}_{mj}\hat{\mathbf{f}}_{jn}^*\hat{\mathbf{f}}_{jn}^T\mathbf{G}_{mj}^H\hat{\mathbf{f}}_{mk}\hat{\mathbf{f}}_{mk}^H\big)\big]$$
$$\overset{(a)}{=}\sum_{n\in\mathcal{U}_d}\sum_{m\in\mathcal{A}_u}\sum_{j\in\mathcal{A}_d}\mathcal{E}_{d,j}\kappa_{jn}^2\mathrm{tr}\big(\mathbb{E}\big[\mathbf{G}_{mj}\hat{\mathbf{f}}_{jn}^*\hat{\mathbf{f}}_{jn}^T\mathbf{G}_{mj}^H\big]\mathbb{E}\big[\hat{\mathbf{f}}_{mk}\hat{\mathbf{f}}_{mk}^H\big]\big)$$
$$= N^2\sum_{m\in\mathcal{A}_u}\sum_{j\in\mathcal{A}_d}\sum_{n\in\mathcal{U}_d}\kappa_{jn}^2\zeta_{mj}\alpha_{mk}^2\alpha_{jn}^2\mathcal{E}_{d,j}.$$

In (a), we apply the linearity of trace. Then we use the fact that $\mathbf{G}_{mj}$ and $\mathbf{f}_{jn}$ are independent, and therefore, $\mathbb{E}[\mathbf{G}_{mj}\hat{\mathbf{f}}_{jn}^*\hat{\mathbf{f}}_{jn}^T\mathbf{G}_{mj}^H] = \zeta_{mj}\mathbb{E}[\mathrm{tr}(\hat{\mathbf{f}}_{jn}^*\hat{\mathbf{f}}_{jn}^T)]\mathbf{I}_N = N\alpha_{jn}^2\zeta_{mj}\mathbf{I}_N$, and $\mathbb{E}[\hat{\mathbf{f}}_{mk}\hat{\mathbf{f}}_{mk}^H] = \alpha_{mk}^2\mathbf{I}_N$, which yields the final result in (9c). ■

Appendix B: Proof of Theorem 2

Proof. We note that from (10), we can write the effective DL SINR as

$$\eta_{d,n} = \big[\big|\sum_{j\in\mathcal{A}_d}\kappa_{jn}\sqrt{\mathcal{E}_{d,j}}\mathbb{E}\big[\mathbf{f}_{jn}^T\hat{\mathbf{f}}_{jn}^*\big]\big|^2\big]$$
$$\times\big(\mathtt{var}\big\{\sum_{j\in\mathcal{A}_d}\kappa_{jn}\sqrt{\mathcal{E}_{d,j}}\mathbf{f}_{jn}^T\hat{\mathbf{f}}_{jn}^*\big\}$$
$$+\sum_{q\in\mathcal{I}_p\backslash n}\mathbb{E}\big[\big|\sum_{j\in\mathcal{A}_d}\kappa_{jq}\sqrt{\mathcal{E}_{d,j}}\mathbf{f}_{jn}^T\hat{\mathbf{f}}_{jq}^*\big|^2\big]$$
$$+\sum_{q\in\mathcal{U}_d\backslash\mathcal{I}_p}\mathbb{E}\big[\big|\sum_{j\in\mathcal{A}_d}\kappa_{jq}\sqrt{\mathcal{E}_{d,q}}\mathbf{f}_{jn}^T\hat{\mathbf{f}}_{jq}^*\big|^2\big]$$
$$+\sum_{k\in\mathcal{U}_u}\mathcal{E}_{u,n}\mathbb{E}\big|\mathtt{g}_{nk}\big|^2 + N_0\big)^{-1}. \tag{27}$$

The gain and the variance of the beamforming uncertainty related terms, i.e., the numerator term and the first term in the denominator of (27), can be obtained via steps similar to those in the UL case. The second term in the denominator of (27), which is the inter-UE interference due to data streams of the UEs that share pilots with the nth UE, i.e., $q\in\mathcal{I}_n\backslash n$, can be expressed as (28). Further algebraic manipulations yield

$$\sum_{q\in\mathcal{I}_p\backslash n}\mathbb{E}\big[\big|\sum_{j\in\mathcal{A}_d}\kappa_{jq}\sqrt{\mathcal{E}_{d,j}}\mathbf{f}_{jn}^T\hat{\mathbf{f}}_{jq}^*\big|^2\big]$$
$$+\sum_{q\in\mathcal{U}_d\backslash\mathcal{I}_p}\mathbb{E}\big[\big|\sum_{j\in\mathcal{A}_d}\kappa_{jq}\sqrt{\mathcal{E}_{d,q}}\mathbf{f}_{jn}^T\hat{\mathbf{f}}_{jq}^*\big|^2\big]$$
$$=N^2\sum_{q\in\mathcal{I}_p\backslash n}\big(\sum_{j\in\mathcal{A}_d}\sqrt{\mathcal{E}_{d,j}}\kappa_{jq}\alpha_{jq}^2\sqrt{\tfrac{\mathcal{E}_{p,n}}{\mathcal{E}_{p,q}}}\tfrac{\beta_{jn}}{\beta_{jq}}\big)^2$$
$$+N\sum_{q\in\mathcal{U}_d\backslash n}\sum_{j\in\mathcal{A}_d}\mathcal{E}_{d,j}\kappa_{jq}^2\beta_{jn}\alpha_{jq}^2. \tag{29}$$

The first term in (29) equates to (12b). The second term together with the nth UE's beamforming uncertainty corresponds to (12a), and (12c) follows from $\mathbb{E}\big|\mathtt{g}_{nk}\big|^2 = \epsilon_{nk}$. ■

Appendix C: Proof of Theorem 3

Proof. We present an inductive proof. Let us assume we schedule the APs in $\mathcal{A}_s$ such that $f_{mk}(\mathcal{A}_s)$ is maximized. Now consider the set $\mathcal{A}_t$, such that $\mathcal{A}_s\subseteq\mathcal{A}_t$. We need to prove that, if we schedule any AP $\{j\}\notin\mathcal{A}_t$ next, the incremental gain obtained by adding $\{j\}$ to $\mathcal{A}_t$ is smaller than the incremental gain achieved by adding $\{j\}$ to $\mathcal{A}_s$. Now, by our hypothesis, the set $\mathcal{A}_s$ is determined first to maximize $f_{mk}(.)$. Therefore, since AP $\{j\}$ is not part of $\mathcal{A}_s$, the product SINR under $\mathcal{A}_s$ is greater than that attained via only activating the $\{j\}$th AP in either of the mode of transmissions, that is, $\prod_{k=1}^K\frac{\sum_{m\in\mathcal{A}_s}\mathtt{G}_{mk}(\mathcal{A}_s)}{\sum_{m\in\mathcal{A}_s}\mathtt{I}_{mk}(\mathcal{A}_s)}\geq\prod_{k=1}^K\frac{\mathtt{G}_{jk}(\{j\})}{\mathtt{I}_{jk}(\{j\})}$. Using the monotonic nondecreasing property in Definition 1, we can write

$$\prod_{k=1}^K\frac{\sum_{m\in\mathcal{A}_t}\mathtt{G}_{mk}(\mathcal{A}_t)}{\sum_{m\in\mathcal{A}_t}\mathtt{I}_{mk}(\mathcal{A}_t)}\geq\prod_{k=1}^K\frac{\sum_{m\in\mathcal{A}_s}\mathtt{G}_{mk}(\mathcal{A}_s)}{\sum_{m\in\mathcal{A}_s}\mathtt{I}_{mk}(\mathcal{A}_s)}$$
$$\Rightarrow\frac{\prod_{k=1}^K\sum_{m\in\mathcal{A}_t}\mathtt{G}_{mk}(\mathcal{A}_t)-\prod_{k=1}^K\sum_{m\in\mathcal{A}_t}\mathtt{G}_{mk}(\mathcal{A}_s)}{\prod_{k=1}^K\sum_{m\in\mathcal{A}_t}\mathtt{I}_{mk}(\mathcal{A}_t)-\prod_{k=1}^K\sum_{m\in\mathcal{A}_s}\mathtt{I}_{mk}(\mathcal{A}_s)}$$
$$\geq\frac{\prod_{k=1}^K\sum_{m\in\mathcal{A}_s}\mathtt{G}_{mk}(\mathcal{A}_s)}{\prod_{k=1}^K\sum_{m\in\mathcal{A}_s}\mathtt{I}_{mk}(\mathcal{A}_s)}\geq\prod_{k=1}^K\frac{\mathtt{G}_{jk}(\{j\})}{\mathtt{I}_{jk}(\{j\})}$$
$$\Rightarrow-\prod_{k=1}^K\mathtt{I}_{jk}(\{j\})\prod_{k=1}^K\sum_{m\in\mathcal{A}_s}\mathtt{G}_{mk}(\mathcal{A}_s)$$
$$+\prod_{k=1}^K\mathtt{G}_{jk}(\{j\})\prod_{k=1}^K\sum_{m\in\mathcal{A}_s}\mathtt{I}_{mk}(\mathcal{A}_s)$$
$$\geq-\prod_{k=1}^K\mathtt{I}_{jk}(\{j\})\prod_{k=1}^K\sum_{m\in\mathcal{A}_t}\mathtt{G}_{mk}(\mathcal{A}_t)$$
$$+\prod_{k=1}^K\mathtt{G}_{jk}(\{j\})\prod_{k=1}^K\sum_{m\in\mathcal{A}_t}\mathtt{I}_{mk}(\mathcal{A}_t) \tag{30}$$

Next, adding and subtracting $\prod_{k=1}^K\sum_{m\in\mathcal{A}_s}\mathtt{G}_{mk}(\mathcal{A}_s)\prod_{k=1}^K\sum_{m\in\mathcal{A}_s}\mathtt{I}_{mk}(\mathcal{A}_s)$ on the left hand side and $\prod_{k=1}^K\sum_{m\in\mathcal{A}_t}\mathtt{G}_{mk}(\mathcal{A}_t)\prod_{k=1}^K\sum_{m\in\mathcal{A}_t}\mathtt{I}_{mk}(\mathcal{A}_t)$ on the right hand side of (30), we get (31), equivalently

$$-\prod_{k=1}^K\sum_{m\in\mathcal{A}_s\cup\{j\}}\mathtt{I}_{mk}(\mathcal{A}_s\cup\{j\})\prod_{k=1}^K\sum_{m\in\mathcal{A}_s}\mathtt{G}_{mk}(\mathcal{A}_s)$$
$$+\prod_{k=1}^K\sum_{m\in\mathcal{A}_s\cup\{j\}}\mathtt{G}_{mk}(\mathcal{A}_s\cup\{j\})\prod_{k=1}^K\sum_{m\in\mathcal{A}_s}\mathtt{I}_{mk}(\mathcal{A}_s)$$

$$\mathbb{E}\big[\big|\sum_{j\in\mathcal{A}_d}\kappa_{jq}\sqrt{\mathcal{E}_{d,j}}\mathbf{f}_{jn}^T\hat{\mathbf{f}}_{jq}^*\big|^2\big]=\mathbb{E}\big[\big|\sum_{j\in\mathcal{A}_d}\kappa_{jq}\sqrt{\mathcal{E}_{d,j}}\tau_p\sqrt{\mathcal{E}_{p,n}\mathcal{E}_{p,q}}c_{jq}\beta_{jq}\|\mathbf{f}_{jn}\|^2\big|^2\big]$$
$$+\mathbb{E}\big[\big|\sum_{j\in\mathcal{A}_d}\kappa_{jq}\sqrt{\mathcal{E}_{d,j}}c_{jq}\sqrt{\tau_p\mathcal{E}_{p,q}}\beta_{jq}\mathbf{f}_{jn}^T\big(\sum_{q'\in\mathcal{I}_p\setminus n}\sqrt{\tau_p\mathcal{E}_{p,q'}}\mathbf{f}_{jq'}+\dot{\mathbf{w}}_{p,j}\big)\big|^2\big]$$
$$=N(N+1)\tau_p^2\mathcal{E}_{p,n}\mathcal{E}_{p,q}\sum_{j\in\mathcal{A}_d}\kappa_{jq}^2\mathcal{E}_{d,j}c_{jq}^2\beta_{jq}^2\beta_{jn}^2+N^2\tau_p^2\mathcal{E}_{p,n}\mathcal{E}_{p,q}\big(\sum_{j\in\mathcal{A}_d}\sqrt{\mathcal{E}_{d,j}}\kappa_{jq}c_{jq}\beta_{jq}\beta_{jn}\big)$$
$$\times\big(\sum_{j'\in\mathcal{A}_d,j'\neq j}\sqrt{\mathcal{E}_{d,j'}}\kappa_{j'q}c_{j'q}\beta_{j'q}\beta_{j'n}\big)+N\tau_p\mathcal{E}_{p,q}\sum_{j\in\mathcal{A}_d}\kappa_{jq}^2\mathcal{E}_{d,j}c_{jq}^2\beta_{jq}^2\big(\sum_{q'\in\mathcal{I}_p\setminus n}\tau_p\mathcal{E}_{p,q'}\beta_{jq'}+N_0\big)\beta_{jn}. \quad (28)$$

$$-\prod_{k=1}^K\big(\mathtt{I}_{jk}(\{j\})+\sum_{m\in\mathcal{A}_s}\mathtt{I}_{mk}(\mathcal{A}_s)\big)\prod_{k=1}^K\sum_{m\in\mathcal{A}_s}\mathtt{G}_{mk}(\mathcal{A}_s)+\prod_{k=1}^K\big(\mathtt{G}_{jk}(\{j\})+\sum_{m\in\mathcal{A}_s}\mathtt{G}_{mk}(\mathcal{A}_s)\big)\prod_{k=1}^K\sum_{m\in\mathcal{A}_s}\mathtt{I}_{mk}(\mathcal{A}_s)$$
$$\geq-\prod_{k=1}^K\big(\mathtt{I}_{jk}(\{j\})+\sum_{m\in\mathcal{A}_t}\mathtt{I}_{mk}(\mathcal{A}_t)\big)\prod_{k=1}^K\sum_{m\in\mathcal{A}_t}\mathtt{G}_{mk}(\mathcal{A}_t)+\prod_{k=1}^K\big(\mathtt{G}_{jk}(\{j\})+\sum_{m\in\mathcal{A}_t}\mathtt{G}_{mk}(\mathcal{A}_t)\big)\prod_{k=1}^K\sum_{m\in\mathcal{A}_t}\mathtt{I}_{mk}(\mathcal{A}_t). \quad (31)$$

$$\geq-\prod_{k=1}^K\sum_{m\in\mathcal{A}_t\cup\{j\}}\mathtt{I}_{mk}(\mathcal{A}_t\cup\{j\})\prod_{k=1}^K\sum_{m\in\mathcal{A}_t}\mathtt{G}_{mk}(\mathcal{A}_t)$$
$$+\prod_{k=1}^K\sum_{m\in\mathcal{A}_t\cup\{j\}}\mathtt{G}_{mk}(\mathcal{A}_t\cup\{j\})\prod_{k=1}^K\sum_{m\in\mathcal{A}_t}\mathtt{I}_{mk}(\mathcal{A}_t).$$

Using the fact that

$$\prod_{k=1}^K\sum_{m\in\mathcal{A}_s\cup\{j\}}\mathtt{I}_{mk}(\mathcal{A}_s\cup\{j\})\prod_{k=1}^K\sum_{m\in\mathcal{A}_s}\mathtt{I}_{mk}(\mathcal{A}_s)$$
$$\leq\prod_{k=1}^K\sum_{m\in\mathcal{A}_t\cup\{j\}}\mathtt{I}_{mk}(\mathcal{A}_t\cup\{j\})\prod_{k=1}^K\sum_{m\in\mathcal{A}_t}\mathtt{I}_{mk}(\mathcal{A}_t),$$

we can finally write,

$$\frac{\prod_{k=1}^K\sum_{m\in\mathcal{A}_s\cup\{j\}}\mathtt{G}_{mk}(\mathcal{A}_s\cup\{j\})}{\prod_{k=1}^K\sum_{m\in\mathcal{A}_s\cup\{j\}}\mathtt{I}_{mk}(\mathcal{A}_s\cup\{j\})}-\frac{\prod_{k=1}^K\sum_{m\in\mathcal{A}_s}\mathtt{G}_{mk}(\mathcal{A}_s)}{\prod_{k=1}^K\sum_{m\in\mathcal{A}_s}\mathtt{I}_{mk}(\mathcal{A}_s)}$$
$$\geq\frac{\prod_{k=1}^K\sum_{m\in\mathcal{A}_t\cup\{j\}}\mathtt{G}_{mk}(\mathcal{A}_t\cup\{j\})}{\prod_{k=1}^K\sum_{m\in\mathcal{A}_t\cup\{j\}}\mathtt{I}_{mk}(\mathcal{A}_t\cup\{j\})}-\frac{\prod_{k=1}^K\sum_{m\in\mathcal{A}_t}\mathtt{G}_{mk}(\mathcal{A}_t)}{\prod_{k=1}^K\sum_{m\in\mathcal{A}_t}\mathtt{I}_{mk}(\mathcal{A}_t)},$$

which reduces to Theorem 3. ■

REFERENCES

[1] H. Q. Ngo, A. Ashikhmin, H. Yang, E. G. Larsson, and T. L. Marzetta, "Cell-free massive MIMO versus small cells," *IEEE Trans. Wireless Commun.*, vol. 16, no. 3, pp. 1834–1850, 2017.

[2] E. Nayebi, A. Ashikhmin, T. L. Marzetta, H. Yang, and B. D. Rao, "Precoding and power optimization in cell-free massive MIMO systems," *IEEE Trans. Wireless Commun.*, vol. 16, no. 7, pp. 4445–4459, 2017.

[3] G. Interdonato, E. Björnson, H. Q. Ngo, P. K. Frenger, and E. G. Larsson, "Ubiquitous cell-free massive MIMO communications," *EURASIP J. Wireless Comm. and Networking*, vol. 2019, p. 197, 2019.

[4] Z. Chen and E. Björnson, "Channel hardening and favorable propagation in cell-free massive MIMO with stochastic geometry," *IEEE Trans Commun.*, vol. 66, no. 11, pp. 5205–5219, 2018.

[5] M. Matthaiou, O. Yurduseven, H. Q. Ngo, D. Morales-Jimenez, S. L. Cotton, and V. F. Fusco, "The road to 6G: Ten physical layer challenges for communications engineers," *IEEE Commun. Mag.*, vol. 59, no. 1, pp. 64–69, 2021.

[6] M. Duarte, C. Dick, and A. Sabharwal, "Experiment-driven characterization of full-duplex wireless systems," *IEEE Trans. Wireless Commun.*, vol. 11, no. 12, pp. 4296–4307, 2012.

[7] M. M. Razlighi, N. Zlatanov, S. R. Pokhrel, and P. Popovski, "Optimal centralized dynamic-time-division-duplex," *IEEE Trans. Wireless Commun.*, vol. 20, no. 1, pp. 28–39, 2021.

[8] G. RP-110450, "Study item description for further enhancements to LTE TDD for DL-UL interference management and traffic adaptation," 2011.

[9] R1-1701616, "Discussion on duplexing flexibility and cross-link interference mitigation schemes," *3GPP TSG RAN WG1 Meeting #88*, Feb. 2017.

[10] R1-1713969, "Discussion on duplexing flexibility and cross-link interference mitigation schemes," *3GPP TSG RAN WG1 Meeting #90*, Aug. 2017.

[11] L. Xue, Y. Cheng, Y. Zhou, and B. Qu, "Next generation TDD cellular communication," in *Proc. Asilomar Conf. on Signals, Syst., and Comput.*, 2015, pp. 1036–1040.

[12] J. Liu, R. Fan, H. Wang, J. Liu, and F. Wang, "Dynamic TDD testbed and field measurements," in *2016 IEEE 83rd Vehicular Technology Conference (VTC Spring)*, 2016, pp. 1–5.

[13] H. Kamboj, B. Anand, S. Gupta, A. Meshram, S. Balijepalli, and C. Murthy, "Hardware implementation of cell-free MIMO and dynamic TDD using the OAI 5G NR codebase," in *25th International ITG Workshop on Smart Antennas*, Eurecom, French Riviera, France, 2021.

[14] H. Kim, J. Kim, and D. Hong, "Dynamic TDD systems for 5G and beyond: A survey of cross-link interference mitigation," *IEEE Commun. Surv. Tutor.*, vol. 22, no. 4, pp. 2315–2348, 2020.

[15] J. Liu, S. Han, W. Liu, and C. Yang, "The value of full-duplex for cellular networks: A hybrid duplex-based study," *IEEE Trans. Commun.*, vol. 65, no. 12, pp. 5559–5573, 2017.

[16] J. Liu, S. Han, W. Liu, Y. Teng, and N. Zheng, "Performance gain of full duplex over half duplex under bidirectional traffic asymmetry," in *Proc. IEEE ICC*, 2016, pp. 98–103.

[17] R1-1702113, "Discussion on duplexing flexibility and cross-link interference mitigation schemes," *3GPP TSG RAN WG1 Meeting #88*, Sophia Antipolis, France, Feb. 2017.

[18] P. Jayasinghe, A. Tölli, J. Kaleva, and M. Latva-aho, "Bi-directional beamformer training for dynamic TDD networks," *IEEE Trans. Signal Process.*, vol. 66, no. 23, pp. 6252–6267, 2018.

[19] D. Wang, M. Wang, P. Zhu, J. Li, J. Wang, and X. You, "Performance of network-assisted full-duplex for cell-free massive MIMO," *IEEE Trans. Commun.*, vol. 68, no. 3, pp. 1464–1478, 2020.

[20] K. Lee, Y. Park, M. Na, H. Wang, and D. Hong, "Aligned reverse frame structure for interference mitigation in dynamic TDD systems," *IEEE Trans. Wireless Commun.*, vol. 16, no. 10, pp. 6967–6978, 2017.

[21] F. Riera-Palou, G. Femenias, A. G. Armada, and A. Pérez-Neira, "Clustered cell-free massive MIMO," in *2018 IEEE Globecom Workshops (GC Wkshps)*, 2018, pp. 1–6.

[22] R. Sabbagh, C. Pan, and J. Wang, "Pilot allocation and sum-rate analysis in cell-free massive MIMO systems," in *Proc. IEEE ICC*, 2018, pp. 1–6.

[23] M. Attarifar, A. Abbasfar, and A. Lozano, "Random vs structured pilot assignment in cell-free massive MIMO wireless networks," in *2018 IEEE International Conference on Communications Workshops (ICC Workshops)*, 2018, pp. 1–6.

[24] E. Björnson and L. Sanguinetti, "Making cell-free massive MIMO competitive with MMSE processing and centralized implementation," *IEEE Trans. Wireless Commun.*, vol. 19, no. 1, pp. 77–90, 2020.

[25] J. Bai and A. Sabharwal, "Asymptotic analysis of MIMO multi-cell full-duplex networks," *IEEE Trans. Wireless Commun.*, vol. 16, no. 4, pp. 2168–2180, April 2017.

[26] T. T. Vu, D. T. Ngo, H. Q. Ngo, and T. Le-Ngoc, "Full-duplex cell-free massive MIMO," in *Proc. IEEE ICC*, 2019, pp. 1–6.

[27] A. Chowdhury, R. Chopra, C. R. Murthy, and H. A. Suraweera, "On the achievable rates of full-duplex massive MIMO systems under channel aging," in *Proc. IEEE SPAWC*, 2019, pp. 1–5.

[28] A. C. Cirik, Y. Rong, and Y. Hua, "Achievable rates of full-duplex MIMO radios in fast fading channels with imperfect channel estimation," *IEEE Trans. Signal Process.*, vol. 62, no. 15, pp. 3874–3886, 2014.

[29] A. Chowdhury, P. Sasmal, and C. R. Murthy, "Comparison of orthogonal vs. union of subspace based pilots for multi-cell massive MIMO systems," in *Proc. IEEE SPAWC*, 2020, pp. 1–5.

[30] M. Bashar, K. Cumanan, A. G. Burr, M. Debbah, and H. Q. Ngo, "On the uplink max–min SINR of cell-free massive MIMO systems," *IEEE Trans. Wireless Commun.*, vol. 18, no. 4, pp. 2021–2036, 2019.

[31] J. Denis and M. Assaad, "Improving cell-free massive MIMO networks performance: A user scheduling approach," *IEEE Trans. Wireless Commun.*, vol. 20, no. 11, pp. 7360–7374, 2021.

[32] E. Björnson, J. Hoydis, and L. Sanguinetti, "Massive MIMO networks: Spectral, energy, and hardware efficiency," *Foundations and Trends® in Signal Processing*, vol. 11, no. 3-4, pp. 154–655, 2017.

[33] Y. Gao, H. Vinck, and T. Kaiser, "Massive MIMO antenna selection: Switching architectures, capacity bounds, and optimal antenna selection algorithms," *IEEE Trans. Signal Process.*, vol. 66, no. 5, pp. 1346–1360, 2018.

[34] S. Fujishige, Ed., *Chapter I - Introduction, Submodular Functions and Optimization*, ser. Annals of Discrete Mathematics. Elsevier, 2005, vol. 58.

[35] S. Ma, L. Xu, C. Du, X. Cheng, and S. Li, "A novel dynamic user admission scheme for multi-cell massive MIMO systems," in *Proc. IEEE Int. Symp. on Broadband Multimedia Systems and Broadcasting (BMSB)*, 2020, pp. 1–4.

[36] R. Vaze and H. Ganapathy, "Sub-modularity and antenna selection in MIMO systems," *IEEE Commun. Lett.*, vol. 16, no. 9, pp. 1446–1449, 2012.

[37] J. Wang, H. Zhu, L. Dai, N. J. Gomes, and J. Wang, "Low-complexity beam allocation for switched-beam based multiuser massive MIMO systems," *IEEE Trans. Wireless Commun.*, vol. 15, no. 12, pp. 8236–8248, 2016.

[38] C. R. Srivatsa and C. R. Murthy, "On the impact of channel estimation on the design and analysis of IRSA based systems," *CoRR*, vol. abs/2112.07242, 2021. [Online]. Available: https://arxiv.org/abs/2112.07242

[39] C. Peel, B. Hochwald, and A. Swindlehurst, "A vector-perturbation technique for near-capacity multiantenna multiuser communication-part I: channel inversion and regularization," *IEEE Trans. Commun.*, vol. 53, no. 1, pp. 195–202, 2005.

[40] J. Zhang, C.-K. Wen, S. Jin, X. Gao, and K.-K. Wong, "Large system analysis of cooperative multi-cell downlink transmission via regularized channel inversion with imperfect CSIT," *IEEE Trans. Wireless Commun.*, vol. 12, no. 10, pp. 4801–4813, 2013.

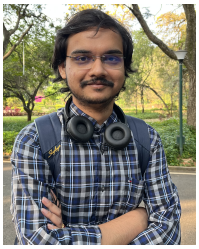

Anubhab Chowdhury (S'21) received the B. Tech. degree in Electronics and Communications Engineering from Jalpaiguri Government Engineering College, West Bengal, India. He has received his M. Tech. degree in Communication Engineering from the Department of Electronics and Electrical Engineering, Indian Institute of Technology, Guwahati, India. He is currently pursuing his Ph. D. in the Department of Electrical Communication Engineering, Indian Institue of Science, Bangalore, India. He is a recipient of the prestigious Prime Minister Research Fellowship since August 2020. His research interests include signal processing and optimization techniques for massive MIMO systems.

Ribhu Chopra (S'11–M'17) received the B.E. degree in Electronics and Communication Engineering from Panjab University, Chandigarh, India in 2009, and the M. Tech. and Ph. D. Degrees in Electronics and Communication Engineering from the Indian Institute of Technology Roorkee, India in 2011 and 2016 respectively. He worked at the Department of Electrical Communication Engineering, Indian Institute of Science, Bangalore, from Aug. 2015, till March 2017. In April 2017, he joined the department of Electronics and Electrical Engineering, Indian Institute of Technology Guwahati, Assam, India. His research interests include statistical and adaptive signal processing, massive MIMO communications, and cognitive communications.

Chandra R. Murthy (S'03–M'06–SM'11) received the B. Tech. degree in Electrical Engineering from the Indian Institute of Technology Madras, India, in 1998, the M. S. and Ph. D. degrees in Electrical and Computer Engineering from Purdue University and the University of California, San Diego, USA, in 2000 and 2006, respectively. In Sept. 2007, he joined the Department of Electrical Communication Engineering at the Indian Institute of Science, Bangalore, India, where he is currently working as a Professor.

His research interests are in the areas of energy harvesting communications, multiuser MIMO systems, and sparse signal recovery techniques applied to wireless communications. His paper won the best paper award in the Communications Track at NCC 2014 and a paper co-authored with his students won the student best paper award at the IEEE ICASSP 2018 and IEEE ISIT 2021. He has 75+ journal papers and 100+ conference papers to his credit. He was an associate editor for the IEEE SIGNAL PROCESSING LETTERS during 2012-16 and for the SADHANA JOURNAL during 2016-18. He was an elected member of the IEEE SPCOM Technical Committee for the years 2014-19. He is currently serving as an area editor for the IEEE TRANSACTIONS ON SIGNAL PROCESSING and as an associate editor for the IEEE TRANSACTIONS ON INFORMATION THEORY and IEEE TRANSACTIONS ON COMMUNICATIONS.